Functional and Effective Connectivity of Effortful Emotion Regulation

FUNCTIONAL AND EFFECTIVE CONNECTIVITY OF EFFORTFUL EMOTION REGULATION

by

Kateri McRae

A Document Submitted to the Faculty of the

DEPARTMENT OF PSYCHOLOGY

In Partial Fulfillment of the Requirements
For the Degree of

DOCTOR OF PHILOSOPHY
WITH A MAJOR IN PSYCHOLOGY

In the Graduate College

THE UNIVERSITY OF ARIZONA

2007

THE UNIVERSITY OF ARIZONA
GRADUATE COLLEGE

As members of the Dissertation Committee, we certify that we have read the dissertation prepared by Kateri McRae

entitled Functional and Effective Connectivity of Effortful Emotion Regulation

and recommend that it be accepted as fulfilling the dissertation requirement for the Degree of Doctor of Philosophy

_____ Date: (April 6, 2007)
(Alfred W. Kaszniak)

_____ Date: (April 6, 2007e)
(Richard D. Lane)

_____ Date: (April 6, 2007)
(John J.B. Allen)

_____ Date: (April 6, 2007e)
(Alan G. Sanfey)

_____ Date: (April 6, 2007)
(A. Randal McIntosh)

Final approval and acceptance of this dissertation is contingent upon the candidate's submission of the final copies of the dissertation to the Graduate College.

I hereby certify that I have read this dissertation prepared under my direction and recommend that it be accepted as fulfilling the dissertation requirement.

_____ Date: (April 6, 2007)
Dissertation Director: (Alfred W. Kaszniak)

STATEMENT BY AUTHOR

This dissertation has been submitted in partial fulfillment of the requirements for an advanced degree at the University of Arizona and is deposited in the University Library to be made available to borrowers under rules of the Library.

Brief quotations from this dissertation are allowable without special permission, provided that accurate acknowledgment of source is made. Requests for permission for extended quotation from or reproduction of this manuscript in whole or in part may be granted by the head of the major department or the Dean of the Graduate college when in his or her judgment the proposed use of the material is in the interests of scholarship. In all other instances, however, permission must be obtained from the author.

SIGNED: Kateri McRae

ACKNOWLEDGEMENTS

I would like to thank and acknowledge my dissertation committee, along with the entire faculty and staff of the Department of Psychology at the University of Arizona. In addition, I would like to extend a special thanks to James Gross and Kevin Ochsner for their collaboration on the fMRI portion of this dissertation. I would like to thank the Stanford Psychophysiology Laboratory for their emotional and scientific support. In addition, thanks to Gary Glover, Peter Sokol-Hessner, Elaine Robertson, Rebecca Ray, Cendri Hutcherson, Supriya Misra, Virginia Favello, Elissa Freedman, Julia Havard, Jessica Donaghy and Anne Yelsey for their varied assistance. This project was also supported by a dissertation grant from the Social and Behavioral Sciences Research Institute at the University of Arizona and by the National Science Foundation.

DEDICATION

To my parents.

TABLE OF CONTENTS

LIST OF FIGURES

LIST OF TABLES

ABSTRACT

Emotion regulation plays an important role in emotional well-being, as well as in the protection against and recovery from mood and anxiety disorders. Previous studies of the functional neuroanatomy of emotion regulation have reported greater activity in prefrontal control-related regions during active regulation. These activations are accompanied by decreases in activity in emotion-responsive regions such as the amygdala and insula. These findings are widely interpreted as consistent with models of cognitive control that implicate top-down, negative influences from prefrontal cortex upon emotion-related processing in other regions. However, no studies to date have used measures of effective connectivity to investigate the likely influence of prefrontal control regions upon emotion-responsive regions in the context of effortful emotion regulation. In the present study, participants alternated between responding naturally to negative emotional stimuli and reinterpreting the negative stimuli with the goal of reducing their experienced negative affect. Functional magnetic resonance imaging (fMRI) was used to measure whole-brain blood-oxygen level dependent signal throughout the task. fMRI data were analyzed using partial least squares (PLS) and structural equations modeling (SEM) to test for differences in effective connectivity between natural and regulated emotional responding. Results indicate that three paths significantly distinguish between regulation and non-regulation negative conditions. The path from inferior frontal gyrus (IFG) to anterior cingulate cortex (ACC) was significantly less positive during regulation than natural responding. In addition, the reciprocal paths between ACC and insula were more negative during regulation than natural responding. Taken as a whole, these

changes in effective connectivity are consistent with assumptions of top-down modulation during effortful emotion regulation. In addition, these changes suggest a pivotal role for the influence of IFG upon ACC and the ACC-insula loop in emotion regulation. The processes represented by these changes and implications for future research are discussed.

INTRODUCTION

The successful regulation of emotion has been implicated in emotional well-being, while failures of emotion regulation may play an important role in mood and anxiety disorders (Campbell-Sills & Barlow, 2007). Although emotion regulation can refer to the up- or down- regulation of positive or negative emotional states using a variety of strategies (Gross, 1998b), the down-regulation of negative emotion using a cognitive emotion regulation strategy is of particular theoretical interest. The cognitive down-regulation of negative emotion is a critical component of cognitive therapy for mood and anxiety disorders (Beck, Rush, Shaw, & Emery, 1979; Bedrosian & Beck, 1980). In addition, the frequent use of cognitive regulation in daily life has been associated with greater well-being and diminished depressive symptoms (Gross & John, 2003). Experimental investigations of the cognitive regulation of emotion have primarily focused on the use of one type of cognitive regulation called reappraisal, defined as the re-interpretation of an emotional stimulus in less emotional terms (Giuliani & Gross, in press). Reappraisal has been associated with decreased emotional responding, as measured by self-reported negative affect, facial expressive behavior, peripheral physiological measures, and neural activity from emotion- responsive regions such as the amygdala and insula (Demaree et al., 2006; Dillon & LaBar, 2005; Eippert, Viet, Weiskopf, Birbaumer, & Anders, in press; Gross, 1998a; Jackson, Malmstadt, Larson, & Davidson, 2000; Ochsner, Bunge, Gross, & Gabrieli, 2002; Ochsner et al., 2004; Phan et al., 2005).

Historically, research on emotion regulation has evaluated the effect of effortful emotion regulation on the magnitude of emotion-related responses such as self-reported emotional experience (Koriat, Melkman, Averill, & Lazarus, 1972) and peripheral physiological measures such as skin conductance (Eippert et al., in press), heart rate (Gross, 1998a; Lazarus, Opton, Nomikos, & Rankin, 1965; Tugade & Fredrickson, 2004) and startle eye-blink response (Eippert et al., in press; Jackson et al., 2000; Ray, McRae, Ochsner, & Gross, under review). However, these physiological measurements do not only measure emotional responding, but also are influenced by cognitive processes involved in regulation, such as attention, imagery and effort (Bradley, Codispoti, & Lang, 2006; Cacioppo & Sandman, 1978; Naccache et al., 2005; Spence, 1972). Therefore, it is not always possible to distinguish the effects of regulation on the emotional response from other consequences of attempted regulation.

The introduction of functional neuroimaging methods has contributed to the study of emotion regulation in two ways. First, activity from regions known to be emotionally responsive such as the amygdala and insula has been considered another dependent variable (used in concert with others) to measure emotional responding (Anderson & Phelps, 2001; Elliot, Rubinsztein, Sahakian, & Dolan, 2000; Phan, Wager, Taylor, & Liberzon, 2002; Schienle et al., 2002; Vaitl, Schienle, & Stark, 2005; Zald, 2003). Several studies have demonstrated that activity in these regions is diminished when participants are instructed to use cognition to down-regulate their negative emotional responses (Ochsner et al., 2002; Ochsner et al., 2004; Phan et al., 2005). Second, a somewhat distinct network of regions has been identified in which activity is greater

during attempted regulation. These regions have been conceptualized as part of a larger network that is engaged during several types of cognitive control (Ochsner & Gross, 2005). These cognitive control regions include the lateral portions of the prefrontal cortex (Jonides, Smith, Marshuetz, Koeppe, & Reuter-Lorenz, 1998; Miyake et al., 2000; Posner & Rothbart, 1998; Yeung, Nystrom, Aronson, & Cohen, 2006) and the anterior cingulate cortex (ACC) (Botvinick, Cohen, & Carter, 2004; di Pellegrino, Ciaramelli, & Ladavas, 2007; Fassbender et al., 2004; Posner & Rothbart, 1998; Weissman, Gopalakrishnan, Hazlett, & Woldorff, 2005).

These regions are typically identified using subtraction-based contrasts (regulate > no regulate and vice versa) and are interpreted as control-related regions exerting top-down inhibition upon emotion-related regions. Several studies have used measures of functional connectivity between the control-related and emotion-responsive regions to confirm this interpretation. These studies indicate that across participants, there is an inverse relationship between activity in control-related and emotion-responsive regions (typically, the amygdala; (Goldin, McRae, Ramel, & Gross, in press; Ochsner et al., 2002; Urry et al., 2006)). Although these findings support the notion that control regions inhibit emotional regions, these approaches have several limitations.

The first limitation is that the subtraction-based contrast approach is not ideally situated to describe functional networks beyond a two-factor model: control-related and emotion-responsive regions. However, it highly possible that cognitive control involves several simultaneous and interacting processes. For example, cognitive control has been conceptualized as engaging at least three types of processes: relatively automatic

processes that are the subject of control, high-level control processes that strategically implement control, and mid-level processes that interface between the two, monitoring the success of the control and signaling the ongoing need for control (Carver & Scheier, 1998). In the case of the cognitive control of emotion, activity in regions involved in planning and strategic goal implementation may represent the control processing, and activity in regions that are known to be involved in cognition-emotion interaction, as well as attention monitoring may represent the mid-level processing. Finally, activity in emotion-responsive regions may represent the relatively automatic processing that is to be controlled.

As mentioned above, the cognitive control literature has focused upon lateral prefrontal regions thought to be involved in the implementation of control (Jonides et al., 1998; Miyake et al., 2000; Posner & Rothbart, 1998; Yeung et al., 2006). It is thought that the anterior cingulate cortex (ACC) performs the proposed monitoring function in concert with these prefrontal regions (Botvinick et al., 2004; Fassbender et al., 2004; Weissman et al., 2005). In addition, the ACC is thought to be engaged during the interaction of emotion and cognition (Bush, Luu, & Posner, 2000; Hutcherson et al., 2005; Lane et al., 1998). There is a substantial amount of theoretical and empirical support for the notion that these two types of control-related regions have distinct but interacting functions in the service of cognitive control (Kerns et al., 2004; Rubia, Smith, Brammer, & Taylor, 2003). However, using only the subtraction-based comparisons mentioned above, the different roles that these regions may play in a network of cognitive control might be obscured. That is, both regions may be identified as more active during

regulation, but only changes in the experimental design or the integration of other measures could begin to differentiate their individual roles in the regulation process.

In addition, the presence of an inverse relationship between control-related regions and emotion-responsive regions does not necessarily confirm a mechanism of top-down control. It is well-known that emotions are not only regulated by cognition, but also that emotion can influence cognition as well (Dolcos, Kragel, Wang, & McCarthy, 2006; Dolcos & McCarthy, 2006). Reports of functional connectivity in various emotional tasks have investigated the nature of the correlation between activity in the amygdala and other regions during emotion-processing tasks. Several studies report differences in functional connectivity between the amygdala and regions that are involved in memory (Canli et al., 2006; Cook, Bookheimer, Mickes, Leuchter, & Kumar, in press; Greenberg et al., 2005; Kilpatrick, Zald, Pardo, & Cahill, 2006; Smith, Stephan, Rugg, & Dolan, 2006) and visual processing (Das et al., 2005; Sabatinelli, Bradley, Fitzsimmons, & Lang, 2005; Williams et al., 2006) in attempts to characterize the influence of the amygdala upon other regions. Therefore, a strong alternative hypothesis is that the inverse functional connection observed between control-related regions and emotion-responsive regions reflects the influence of the latter upon the former.

Lastly, these functional “connections” are not necessarily supported by direct anatomical connections between regions, and so these findings are limited in their interpretability. In contrast to functional connectivity, models that incorporate known anatomical connectivity between regions are referred to as investigating effective connectivity (Friston, 1994; McIntosh & Gonzales-Lima, 1994). Because there are no

known direct efferent connections from the prefrontal regions usually observed in the cognitive control of emotion and the amygdala, if a prefrontal inhibitory influence is present, it must travel through some other node in the network. Alternately, there is a direct efferent connection from the amygdala to some lateral prefrontal regions (Porrino, Crane, & Goldman-Rakic, 1981), so it is possible that the inverse relationship observed previously is the result of the influence of the amygdala on prefrontal regions. Reports from subtraction-based contrasts or functional connectivity analyses cannot distinguish between these possible patterns of effective connectivity.

One method of investigating effective connectivity is to use structural equation modeling (SEM) and functional covariation between regions to create models that are constrained by known anatomical connections (McIntosh & Gonzales-Lima, 1994; Penny, Stephan, Mechelli, & Friston, 2004). A potential concern with this approach is that SEM, as used in the behavioral sciences, requires a sample size much greater than typical neuroimaging studies allow (several hundred participants). However, the large sample sizes are required to confirm models when directional influences are not derived independently of the data. Simulations have demonstrated that even when traditional fit indices do not indicate that the models account for the correlations observed in the data, differences between experimental conditions or groups can be detected reliably (McIntosh, 1999; Protzner & McIntosh, 2006). Therefore, these approaches are informative about differences in effective connectivity between experimental conditions or groups.

The aim of the present study was to replicate previous reports of an inverse functional relationship between prefrontal control regions and emotion-responsive regions during the effortful regulation of negative emotion. In addition, the present study was meant to extend this aim by investigating differences in effective connectivity between the regulation and non-regulation conditions. The effective connectivity models employed here can provide support for the directionality of the inverse relationship mentioned above. In addition, these models can identify mediating structures through which prefrontal regions may have their effect on emotion-responsive regions.

The present study used a multi-step approach to identify changes in effective connectivity during the cognitive regulation of negative emotion. First, a multivariate neuroimaging analysis technique (partial least squares; PLS) was used to identify regions that significantly covary with one another and vectors representing the current experimental design. The experimental task involved viewing negative and neutral pictures from the international affective picture system (IAPS; Lang, Bradley, & Cuthbert, 2001) under two instructional conditions: one to look and respond naturally, and one to decrease the amount of negative affect experienced during the picture using cognitive reappraisal. Because amygdala activity is known to distinguish between negative and neutral stimuli (Phan et al., 2002; Zald, 2003) and is down-regulated by cognitive reappraisal (Ochsner et al., 2002; Ochsner et al., 2004; Phan et al., 2005), it is hypothesized that activity in the amygdala will reliably distinguish between negative and neutral picture-viewing conditions. Should that be confirmed, regions that significantly covary (positively and negatively) with amygdala activity during the task will be

identified using peak values from the amygdala in a seed analysis. Based on the previous literature on negative emotion and known anatomical connectivity between regions, SEM will be used to identify significant differences in effective connectivity during the different experimental conditions.

It is hypothesized that control-related regions will be identified in the multivariate analyses that will distinguish between the regulation and non-regulation conditions. The influence of these cognitive control regions upon the amygdala (and other emotion-responsive regions) is hypothesized to be more strongly negative during the cognitive regulation than the non-regulation condition.

PRESENT STUDY

Participants

Twenty-five participants (12 women; mean age = 20.55, standard deviation = 1.49) were recruited for participation in the present study. Potential participants were screened via email for eligibility and were excluded from participation due to: left-handedness, age below 18 and above 22, native language other than English, current or past diagnosis of neurological or psychiatric disorder, history of head trauma, pregnancy, current use of psychoactive medication, or any non-MRI compatible conditions (e.g., metal in body, tattoo on face or neck, pregnancy, medicine delivery patch). Participants provided their written informed consent, were compensated for their participation, and were studied under the guidelines of the IRBs at Stanford University and the University of Arizona.

Task

The trial structure was as follows: an instruction word was presented in the middle of the screen (“decrease” or “look”; 4 seconds), a picture was presented (negative if instruction was decrease (regulation instruction), negative or neutral if instruction was look (non-regulation instruction; 8 seconds), followed by a rating period (scale from 1-4; 4 seconds) and then the word “relax”(4 seconds; see Figure 1). The 8-second picture presentation period was the only trial section modeled in the neuroimaging analyses presented here. A total of 90 trials (30 of each trial type) were administered in 4 runs of

22 or 23 trials each. Stimuli were presented and button responses collected using Psyscope software (Cohen, MacWhinney, Flatt, & Provost, 1993) running on a Macintosh G3 computer. An LCD projector displayed stimuli on a screen mounted on a custom head coil fitted with a bite-bar to limit head motion.

Figure 1. Schematic of experimental task.

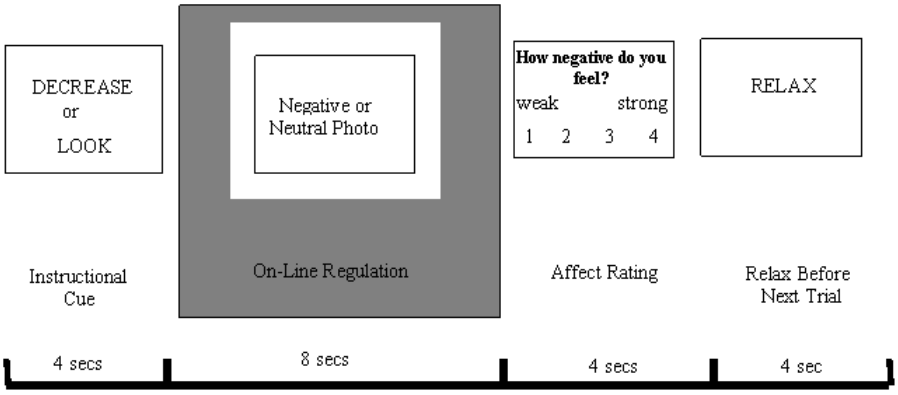

Picture stimuli were taken from the IAPS. Pictures were randomized into four different picture presentation orders to reduce the effect of idiosyncratic assignment of picture to instruction and picture order. Within each order, pictures were counterbalanced into the look negative and the decrease negative conditions such that normative valence and arousal ratings did not differ between the two conditions (see Appendix B). Instruction and picture types were pseudo- randomized with the constraint that no more than three of any trial type or picture type followed each other sequentially.

Prior to any task training, participants were given written instructions for the experiment. After reading the instructions, participants completed a practice session during which the experimenter showed sample negative and neutral images not used in

the experiment. For the regulation (decrease) trials, the experimenter prompted the participant to narrate aloud his or her self-generated re-interpretation of the image. Re-interpretations were limited to three categories: 1) It's not real (e.g., it's just a scene from a movie, they're just pretending) 2) Things will improve with time (e.g., whatever is going wrong will resolve over time) 3) Things aren't as bad as they appear to me (e.g., the situation looks worse than it is, it could be a lot worse, at least it's not me in that situation). Any reports that participants were using a non-cognitive strategy (such as distraction or expressive suppression) were corrected and participants were re-directed to use one of the three strategies mentioned above.

Brain Imaging

Functional Imaging

Twenty-five axial slices (4 mm thick, 1mm skip) were collected at a 3T (GE Signa LX Horizon Echospeed) scanner with a T2* sensitive gradient echo spiral-in-out pulse sequence (TR= 2.00, TE= 30ms, 60° flip angle, 24-cm field of view, 64 x 64 data acquisition matrix) which has been shown to effectively reduce signal dropout at high field strengths. Evaluation of signal dropout in medial temporal and orbitofrontal regions revealed that signal retained was equal to or better than previous reports using this sequence (Preston, Thomason, Ochsner, Cooper, & Glover, 2004). Two hundred thirty whole-brain images were taken in each of four 7-minute, 40-second runs.

Anatomical Imaging

T2-weighted flow-compensated spin echo scans were acquired for anatomical localization using identical slice prescription as the functional scans.

Self-reported affect

Following presentation of each picture, participants were prompted to answer the question “How negative do you feel?” on a scale from 1 to 4 (4 labeled “strong”, 1 labeled “weak”). Responses were made on a 4-button button box using the participant’s dominant (right) hand.

Skin conductance acquisition

Skin conductance responses (SCRs) were collected simultaneously with functional imaging using two Ag/AgCl electrodes filled with an electrolyte of sodium chloride in Unibase placed on the second and fourth fingers of the non-dominant (left) hand and a PowerLab galvanic skin response amplifier (ML116, ADInstruments, Colorado Springs, CO). Data were sampled at 40 Hz.

Data Analysis

Manipulation check

Several measures were collected to determine whether a greater amount of negative affect was induced in the look negative than the decrease negative and look neutral conditions. This was assessed by independently examining participants’ self-

reported affect, skin conductance response and the subtraction-based contrasts from the functional imaging data.

Self-reported affect

Mean affect ratings were calculated for the look negative, look neutral, and decrease negative conditions. A repeated-measures general linear model (GLM) was performed using Statistical Package for the Social Sciences version 15 (SPSS; Chicago, IL) to ensure that negative pictures elicited higher ratings of negative affect than neutral pictures, and that negative pictures viewed under the decrease instruction elicited less negative affect than those viewed under the look instruction.

Skin conductance response

Due to experimenter error and malfunction of the trigger signal from the scanner to the SCR recording computer, skin conductance responses were only recorded for 21 of the 24 participants. Unfortunately, due to noise induced by the scanner and SCR non-responsivity, no participant displayed score-able SCRs during picture-viewing on more than 10% of the trials. Therefore, SCR data is not reported here.

Basic Contrasts

Each participant's sequential functional volumes were realigned to the first scan and co-registered to his or her anatomical MRI using an automated rigid-body transformation algorithm using statistical parametric mapping software (SPM2; Wellcome Department of Neurology, London, UK). Default SPM2 settings were used to warp volumetric MRIs to fit a standardized template (16 non-linear iterations), and normalization parameters were applied to subjects' co-registered functional images.

Normalized images were resampled into 2 x 2 x 2 mm voxels. One participant (male) was removed from all analyses due to motion greater than 3 mm over the course of the four scans. Behavioral data reported here also excludes this participant. Finally, images were smoothed with a 6 mm full width at half maximum kernel. Preprocessed images were entered into a GLM in SPM that modeled the canonical hemodynamic response function convolved with an 8-second boxcar representing the picture-viewing period. These models were used to create subtraction contrasts between conditions of interest (look negative > look neutral, decrease negative > look negative and its inverse) for each subject. These individual contrasts were then entered into a one-sample t-test to perform a random-effects group analysis. Unless otherwise noted, group-level results result from a display threshold of $p<0.001$, uncorrected.

PLS

Pre-processed images were entered into PLS software (McIntosh, Bookstein, Haxby, & Grady, 1996). PLS is a multivariate data analysis technique that identifies patterns of covariation between brain imaging data and vectors provided by the user. In the most basic case, vectors can represent the different conditions of the experiment (referred to as a task PLS). In addition, vectors can represent behavioral data or an individual difference measure for each subject (referred to as a behavior PLS). Lastly, one can extract the data from any voxel or cluster and use it in a behavioral PLS to estimate functional connectivity from the chosen voxel (referred to as a seed PLS). PLS analyses yield latent variables (LVs) that consist of a pattern of positive and negative covariation across the brain and a weighting on the covariate vector (task, behavioral or

seed). In addition, brain scores are computed for each participant that indicate the degree to which that participant's data is consistent with each LV. One participant (female) was removed from the PLS analysis due to extreme brain scores (greater than 5 standard deviations from the group mean). For all PLS analyses reported here, the significance of each LV was assessed with a permutation test (100 iterations) in which the conditions were randomly assigned across participants. Each voxel's reliable contribution to the LVs was evaluated by computing a ratio of each voxel's salience to its standard error via bootstrap estimation (resampling with replacement; 50 iterations). Unless noted otherwise, the reported clusters were identified as 5 contiguous voxels (with a 10 mm minimum distance between peaks) with a minimum bootstrap ratio having a probability < 0.001.

SEM

A subset of the clusters identified in the seed PLS were chosen for inclusion in the SEMs. The results section and Appendix A provide detailed region selection criteria. Values from peak voxels in the chosen clusters were extracted and separate correlation matrices were computed for each condition. The correlation matrices were entered into stacked models in LISREL 8.8 (Scientific Software International, Inc. Lincolnwood, IL, 2004). A stacked model evaluates the relative fit of models that are free or constrained across conditions. A free model allows a given path to have a different value in conditions A and B, whereas a constrained model specifies that the value of a given path is the same in both conditions. Differential model fit was evaluated using the difference

in χ^2 and the difference in degrees of freedom between the free and constrained models. If the models differed significantly, each path was tested one at a time to identify the paths that contributed most strongly to the differential model fit. To reduce the number of variables in the model, and to make better use of anatomical connectivity data (which is primarily done using ipsilateral connections), regions from only one hemisphere (right) were tested. This approach has been used before (de Marco, de Bonis, Vrignaud, Henry-Feugeas, & Peretti, 2006), and is particularly appropriate given mixed reports on hemispheric differences in emotional processing (Cahill, Uncapher, Kilpatrick, Alkire, & Turner, 2004; Thibodeau, Jorgensen, & Kim, 2006; Wager, Phan, Liberzon, & Taylor, 2003). The right hemisphere was tested because right amygdala activity is more commonly down-regulated in studies of the cognitive control of emotion (Ochsner et al., 2002) and because only the right amygdala was identified in the task PLS in the present study.

RESULTS

Manipulation check

Self-reported affect

A repeated measures GLM performed upon mean ratings of negative affect revealed differences between all three conditions ($F(2, 22) = 198.188$, $p<0.001$). Consistent with previous reports (Gross, 1998a; Ochsner et al., 2002; Ray et al., under review), participants reported feeling most negative during the look negative condition, significantly less negative during the decrease negative condition, and significantly least negative during the look neutral condition (all pairwise comparisons $p<0.001$, Figure 2).

Figure 2. Mean ratings of negative affect by condition. '4' represents "strong negative feeling" and "1" represents "weak negative feeling.

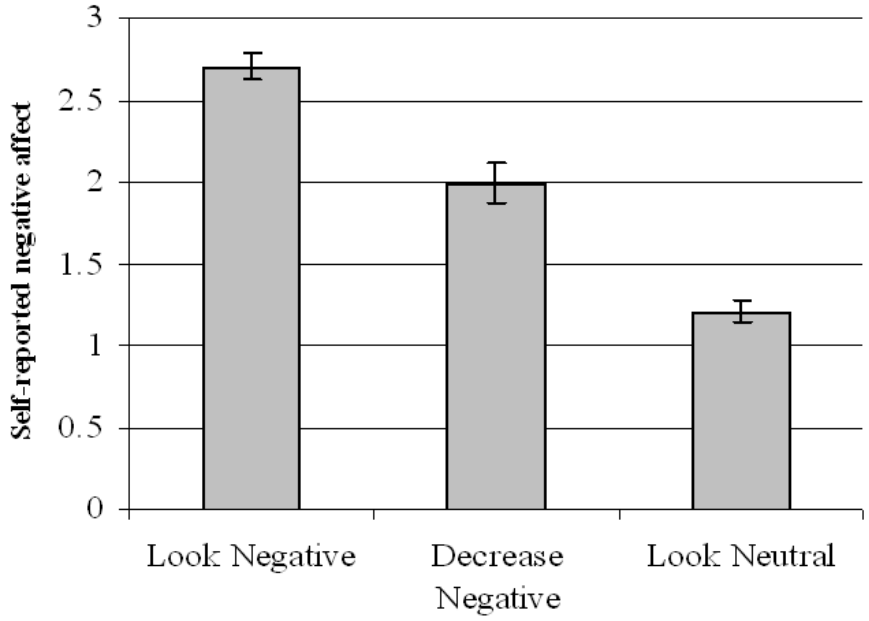

Basic Contrasts

Second-level contrasts in SPM were created comparing the picture-viewing period during conditions of interest (look negative> look negative, decrease negative> look negative, look negative > decrease negative). Regions that showed significantly greater activation for the look negative >look neutral contrast can be found in Table 1 and Figure 3. Greater activity was observed during the look negative condition in several visual areas, superior temporal gyri, several prefrontal areas, and one apriori region of interest (bilateral amygdala).

Figure 3. Look negative > look neutral second-level contrast in SPM. Threshold was set to $p<0.001$, uncorrected. Anatomical underlay is a single-subject (not from the present study) T1 image warped to fit a normalized template.

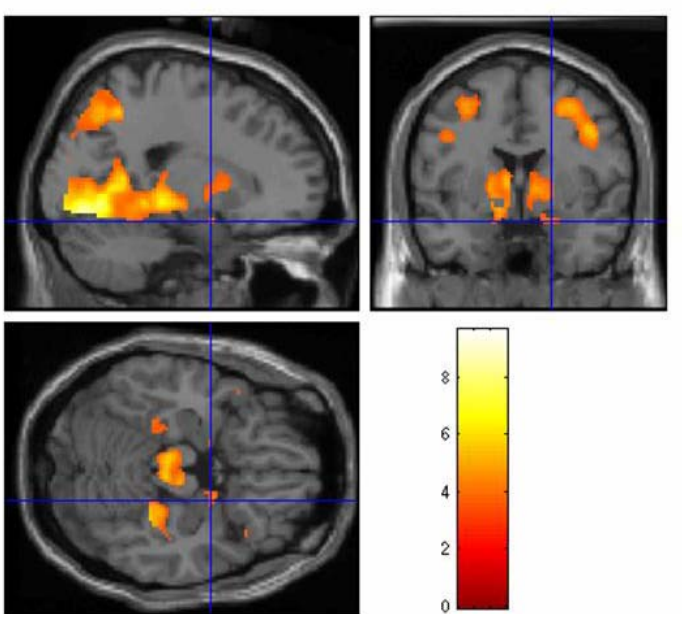

Table 1. Clusters from SPM second-level analysis (one-sample t-test). Look Negative > Look Neutral. Threshold was p<0.001, uncorrected. XYZ values represent MNI coordinates. B.A. = Brodmann area. Region labels from Talairach Daemon.

X	Y	Z	Cluster Size	Z score	p uncorr	B.A.	Region	Type
-30	-50	-14	18788	6.04	<0.001	B.A. 37	Fusiform Gyrus	Occipital
44	8	30	1990	5.79	<0.001	B.A. 9	Inferior Frontal Gyrus	Frontal
-32	26	0	1261	5.28	<0.001	B.A. 47	Inferior Frontal Gyrus	Frontal
-4	18	54	2373	4.92	<0.001	B.A. 8	Superior Frontal Gyrus	Frontal
36	26	-2	181	4.49	<0.001	B.A. 47	Inferior Frontal Gyrus	Frontal
-34	-6	50	299	4.11	<0.001	B.A. 6	Middle Frontal Gyrus	Frontal
40	22	-18	4	3.34	<0.001	B.A. 47	Inferior Frontal Gyrus	Frontal
-44	14	-22	23	3.28	0.001	B.A. 38	Superior Temporal Gyrus	Temporal
-6	10	26	8	3.26	0.001	B.A. 33	Anterior Cingulate	Limbic
42	26	-14	4	3.23	0.001	B.A. 47	Inferior Frontal Gyrus	Frontal
56	34	4	1	3.18	0.001	N/A	Inferior Frontal Gyrus	Frontal
32	14	-22	1	3.11	0.001	N/A	Superior Temporal Gyrus	Temporal
-16	62	24	1	3.1	0.001	B.A. 10	Superior Frontal Gyrus	Frontal
-8	38	28	2	3.09	0.001	N/A	Anterior Cingulate	Limbic

Regions that showed significantly greater activation for the decrease negative > look negative contrast can be found in Table 2 and Figure 4. Greater activity was observed during the decrease negative condition in bilateral frontal regions, as well as superior temporal areas and midline anterior cingulate regions. Regions that showed significantly greater activation for the look negative > decrease negative contrast can be found in Table 3 and Figure 5. In addition to greater left insula activity at the wholebrain threshold, greater activity was observed in the right amygdala for the look negative > decrease negative contrast after a small volume correction (21 voxels, peak at [24 0 -18], $p< 0.019$, $Z =2.07$) and a small cluster in the left amygdala (3 voxels, peak at [-20 2 -18], $p<0.039$, $Z=1.76$).

Figure 4. Decrease negative > look negative second-level contrast in SPM. Threshold was $p<0.001$, uncorrected. Anatomical underlay is a single-subject (not from the present study) T1 image warped to fit a normalized template.

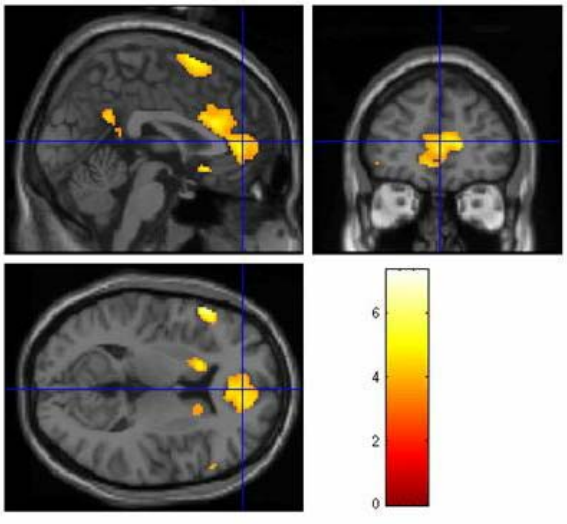

Table 2. Clusters from SPM second-level analysis (one-sample t-test). Decrease Negative > Look Negative. Threshold was p<0.001, uncorrected. XYZ values represent MNI coordinates. B.A. = Brodmann area. Region labels from Talairach Daemon.

X	Y	Z	Cluster Size	Z score	p uncorr	B.A.	Region	Lobe
-56	20	14	525	5.23	<0.001	B.A.45	Inferior Frontal Gyrus	Frontal
-10	10	70	2694	4.93	<0.001	B.A.6	Superior Frontal Gyrus	Frontal
-48	-66	36	763	4.86	<0.001	B.A.39	Inferior Parietal Lobule	Parietal
-16	16	8	191	4.27	<0.001	Caudate Body	Caudate	Sub-lobar
-2	-52	28	356	4.24	<0.001	B.A.31	Cingulate Gyrus	Limbic
50	30	-10	437	4.2	<0.001	B.A.47	Inferior Frontal Gyrus	Frontal
20	14	20	124	4.15	<0.001	Caudate Body	Caudate	Sub-lobar
-42	4	46	241	4.11	<0.001	B.A.6	Middle Frontal Gyrus	Frontal
-58	-8	-18	62	4.02	<0.001	B.A.21	Inferior Temporal Gyrus	Temporal
58	-58	28	121	3.97	<0.001	B.A.39	Superior Temporal Gyrus	Temporal
2	18	-10	38	3.85	<0.001	N/A	Anterior Cingulate	Limbic
-62	-40	-6	86	3.84	<0.001	B.A.21	Middle Temporal Gyrus	Temporal
50	-36	4	38	3.52	<0.001	B.A.22	Superior Temporal Gyrus	Temporal
-6	34	60	8	3.37	<0.001	N/A	N/A	N/A
-18	22	56	16	3.31	<0.001	B.A.8	Superior Frontal Gyrus	Frontal
-8	-6	-16	6	3.29	<0.001	N/A	N/A	N/A
46	6	48	8	3.26	0.001	B.A.8	Middle Frontal Gyrus	Frontal
-2	-22	34	8	3.21	0.001	B.A.23	Cingulate Gyrus	Limbic
56	14	2	2	3.2	0.001	N/A	N/A	Frontal-Temporal Space
16	-18	-16	3	3.18	0.001	N/A	N/A	Midbrain
-12	38	-8	1	3.11	0.001	B.A.10	Medial Frontal Gyrus	Frontal
-22	26	48	1	3.11	0.001	B.A.8	Superior Frontal Gyrus	Frontal
-18	2	22	2	3.11	0.001	Caudate Body	Caudate	Sub-lobar
60	-32	-10	1	3.09	0.001	B.A.21	Middle Temporal Gyrus	Temporal

Figure 5. Look negative > decrease negative second-level contrast in SPM. Threshold was p<0.001, uncorrected (a) and p<0.05 uncorrected (b) to search an apriori region of interest (bilateral amygdala). Anatomical underlay is a single-subject (not from the present study) T1 image warped to fit a normalized template.

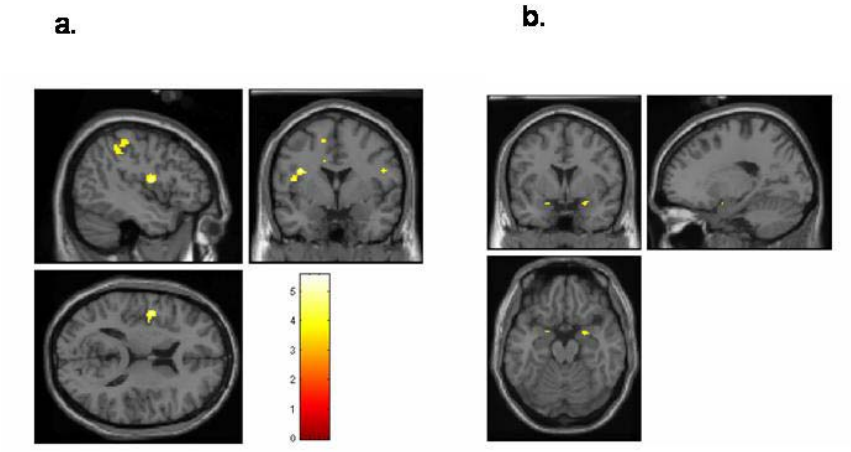

Table 3. Clusters from SPM second-level analysis (one-sample t-test). Look Negative > Decrease Negative. Threshold was p<0.001, uncorrected. XYZ values represent MNI coordinates. B.A. = Brodmann area. Region labels from Talairach Daemon.

X	Y	Z	Z score	Cluster Size	p uncorr	B.A.	Region	Lobe
-36	0	24	4.39	160	<0.001	B.A. 6	Precentral Gyrus/ Insula	Frontal
-52	-32	38	4.25	707	<0.001	B.A. 2	Postcentral Gyrus	Parietal
38	-48	42	4.09	85	<0.001	B.A. 40	Inferior Parietal Lobule	Parietal
-14	-48	64	3.95	66	<0.001	B.A. 7	Precuneus	Parietal
-14	-8	52	3.87	75	<0.001	B.A. 24	Cingulate Gyrus	Limbic
50	-20	32	3.68	9	<0.001	B.A. 2	Postcentral Gyrus	Parietal
-20	-26	52	3.68	20	<0.001	B.A. 3	Postcentral Gyrus	Frontal
-40	-38	34	3.65	13	<0.001	B.A. 40	Inferior Parietal Lobule	Parietal
-36	-46	4	3.61	14	<0.001	N/A	Sub-Gyral	Temporal
-30	-14	58	3.54	32	<0.001	B.A. 6	Precentral Gyrus	Frontal
-28	-36	10	3.53	13	<0.001	Caudate Tail	Caudate	Sub-lobar
50	0	24	3.39	5	<0.001	B.A. 9	Inferior Frontal Gyrus	Frontal
38	-32	54	3.38	9	<0.001	B.A. 3	Postcentral Gyrus	Parietal
-22	-40	48	3.27	4	0.001	B.A. 5	Paracentral Lobule	Frontal
-40	-22	-6	3.26	6	0.001	B.A. 22	Superior Temporal Gyrus	Temporal
-12	0	34	3.12	1	0.001	B.A. 24	Cingulate Gyrus	Limbic
-60	2	22	3.09	1	0.001	B.A. 6	Precentral Gyrus	Frontal

PLS

Participants' functional images were entered into a task PLS to create LVs that represent the covariance between the fMRI data and the three experimental conditions. Only the picture presentation period was considered, and the first scan of each trial was used as a reference scan. Only the first LV reliably explained a significant portion of the covariance in the brain-task block ($p<0.001$). This LV distinguished between the negative pictures (regardless of instructional condition) and the neutral pictures (see Figures 6 and 7 and Table 4).

Figure 6. Experimental task condition weightings on LV1 for Task PLS. Conditions are depicted in the following order: look neutral, look negative, decrease negative.

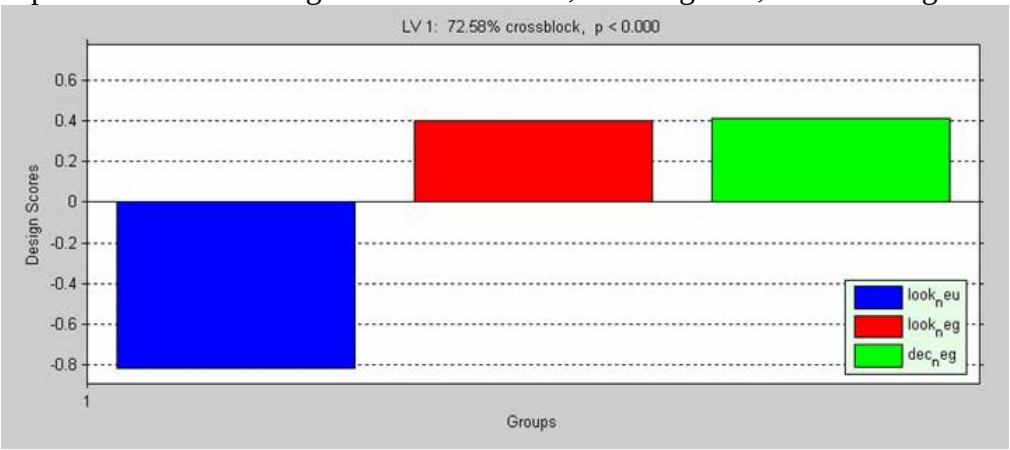

Figure 7. LV1 for Task PLS, displayed over normalized T1-weighted anatomical image. Lags (TRs) 0-4 are depicted in the descending rows.

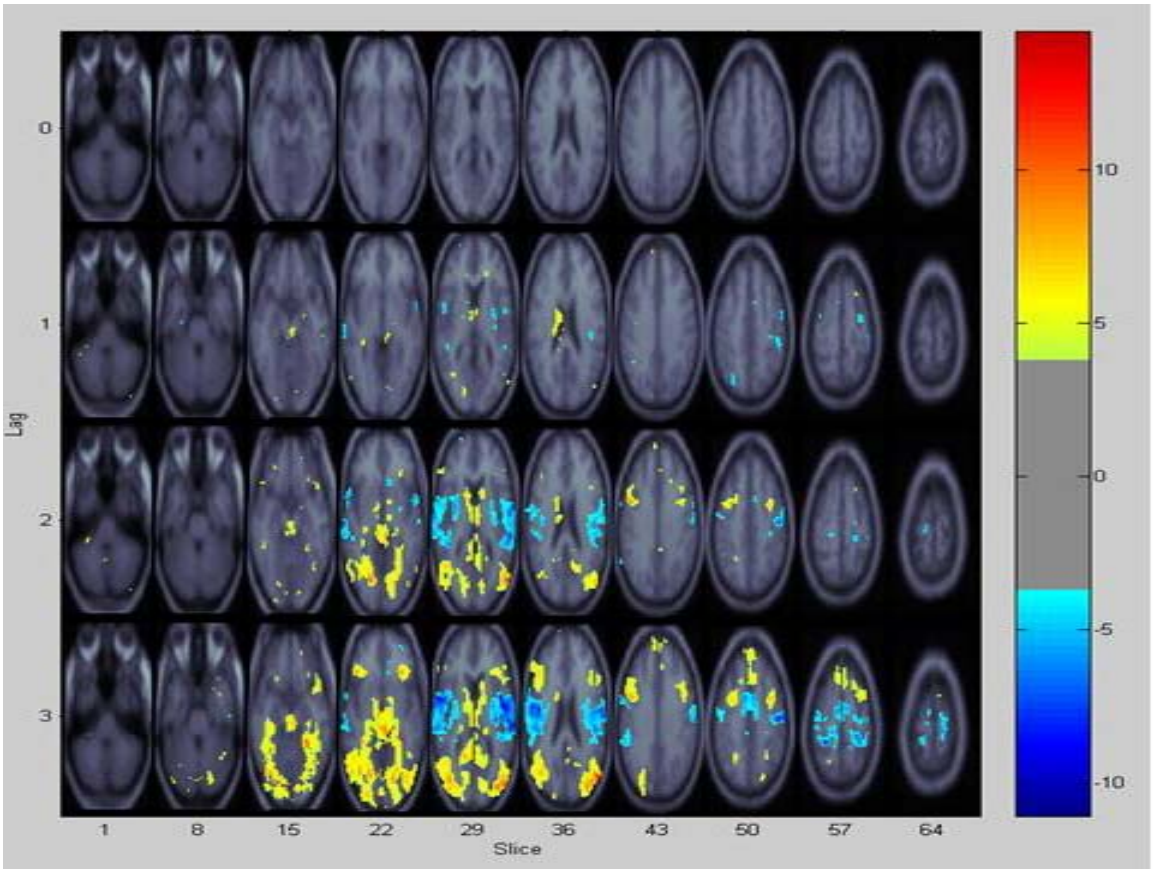

Table 4. Clusters with p<0.0001 from LV1, Task PLS, Study 2. XYZ values represent MNI coordinates. B.A. = Brodmann Area. BSR= bootsrap ratio. Region labels from Talairach Daemon. a. Lag 1 b. Lag 2 c. Lag 3.

a.

X	Y	Z	BSR	Cluster Size	B.A.	Region	Lobe
-20	-24	20	8.25	219	Caudate Tail	Caudate	Sub-lobar
-4	-22	14	7.36	314	N/A	Thalamus	Sub-lobar
8	-30	-8	6.12	164	N/A	N/A	Midbrain
4	36	54	5.98	70	B.A. 8	Superior Frontal Gyrus	Frontal
24	10	56	5.66	60	B.A. 6	Superior Frontal Gyrus	Frontal
-36	-66	6	5.60	30	B.A. 19	Middle Occipital Gyrus	Occipital
20	-16	-10	5.47	11	N/A	N/A	Midbrain
-32	-36	-4	5.31	30	N/A	Lateral Ventricle	Sub-lobar
-38	-26	-16	5.25	20	B.A. 36	Parahippocampal Gyrus	Limbic
38	2	52	5.09	23	B.A. 6	Middle Frontal Gyrus	Frontal
10	-82	-18	5.07	29	N/A	Declive	Cerebellum
54	-76	2	4.97	45	B.A. 19	Middle Occipital Gyrus	Occipital
-42	-46	-14	4.86	13	B.A. 37	Sub-Gyral	Temporal
-18	-80	4	4.75	28	B.A. 17	Cuneus	Occipital
4	-2	2	4.74	35	N/A	Thalamus	Sub-lobar
22	-10	-20	4.71	9	B.A. 34	Parahippocampal Gyrus	Limbic
-2	6	-12	4.68	8	B.A. 25	Anterior Cingulate	Limbic
-10	-32	22	4.63	21	B.A. 23	Posterior Cingulate	Limbic
-50	-76	0	4.56	20	B.A. 19	Middle Occipital Gyrus	Occipital
10	-46	26	4.50	23	B.A. 31	Cingulate Gyrus	Limbic
36	-42	0	4.41	8	N/A	Lateral Ventricle	Sub-lobar
-4	-32	-26	4.40	10	N/A	N/A	Pons
-26	-64	-2	4.40	11	B.A. 19	Lingual Gyrus	Occipital
20	32	8	4.38	15	N/A	Sub-Gyral	Frontal
52	-66	8	4.33	6	B.A. 39	Middle Temporal Gyrus	Temporal
14	-64	28	4.31	6	B.A. 31	Precuneus	Occipital
-18	-10	8	4.27	11	Putamen	Lentiform Nucleus	Sub-lobar
6	-32	26	4.24	8	B.A. 23	Posterior Cingulate	Limbic
-6	-16	40	4.21	8	B.A. 24	Cingulate Gyrus	Limbic
46	-76	24	4.17	21	B.A. 39	Middle Temporal Gyrus	Temporal
24	-12	22	4.07	10	N/A	Thalamus	Sub-lobar
24	14	0	-8.59	61	Putamen	Lentiform Nucleus	Sub-lobar

46	-32	60	-6.41	313	B.A. 2	Postcentral Gyrus	Parietal
54	-8	46	-6.40	86	B.A. 4	Precentral Gyrus	Frontal
-66	-26	-6	-6.35	149	B.A. 21	Middle Temporal Gyrus	Temporal
-54	2	0	-5.99	113	N/A	Superior Temporal Gyrus	Temporal
26	-16	74	-5.56	92	B.A. 6	Precentral Gyrus	Frontal
-24	20	2	-5.55	45	N/A	Claustrum	Sub-lobar
-26	-76	50	-5.51	60	B.A. 7	Precuneus	Parietal
-6	4	60	-5.37	13	B.A. 6	Superior Frontal Gyrus	Frontal
32	-4	6	-5.32	48	Putamen	Lentiform Nucleus	Sub-lobar
-46	-38	6	-5.28	38	B.A. 22	Superior Temporal Gyrus	Temporal
58	0	-8	-5.16	79	B.A. 21	Middle Temporal Gyrus	Temporal
46	-30	16	-5.02	77	B.A. 41	Superior Temporal Gyrus	Temporal
26	-14	52	-5.00	25	B.A. 6	Precentral Gyrus	Frontal
54	-14	-4	-5.00	14	B.A. 22	Superior Temporal Gyrus	Temporal
6	2	60	-4.78	64	N/A	Superior Frontal Gyrus	Frontal
-36	-8	64	-4.74	26	N/A	Middle Frontal Gyrus	Frontal
52	-40	6	-4.74	24	B.A. 22	Superior Temporal Gyrus	Temporal
18	34	-12	-4.63	35	B.A. 47	Inferior Frontal Gyrus	Frontal
62	-28	0	-4.60	27	N/A	Middle Temporal Gyrus	Temporal
36	-20	4	-4.29	9	N/A	Claustrum	Sub-lobar
36	-30	48	-4.26	8	B.A. 2	Postcentral Gyrus	Parietal
-62	-34	14	-4.20	6	B.A. 22	Superior Temporal Gyrus	Temporal
-62	10	38	-4.15	7	N/A	Inferior Frontal Gyrus	Frontal
-62	2	12	-4.09	8	B.A. 6	Precentral Gyrus	Frontal
-42	28	0	-4.07	7	B.A. 47	Inferior Frontal Gyrus	Frontal

b.

X	Y	Z	BSR	Cluster Size	B.A.	Region	Lobe
-18	-74	-6	10.97	2981	B.A. 18	Lingual Gyrus	Occipital
56	-74	6	10.53	1369	B.A. 19	Middle Occipital Gyrus	Occipital
-48	2	34	9.61	811	B.A. 9	Inferior Frontal Gyrus	Frontal
6	-16	10	9.46	2338	Medial Dorsal Nucleus	Thalamus	Sub-lobar
-6	-16	12	8.07	656	Medial Dorsal Nucleus	Thalamus	Sub-lobar
42	-62	-20	7.78	67	B.A. 37	Fusiform Gyrus	Temporal
26	-68	-10	7.70	1605	B.A. 19	Fusiform Gyrus	Occipital
40	26	14	6.69	154	B.A. 13	Inferior Frontal Gyrus	Frontal

38	2	54	6.52	596	B.A. 6	Middle Frontal Gyrus	Frontal
-54	30	10	5.80	104	B.A. 46	Inferior Frontal Gyrus	Frontal
46	12	-26	5.78	82	B.A. 38	Superior Temporal Gyrus	Temporal
-16	-94	-18	5.51	28	B.A. 17	Lingual Gyrus	Occipital
-24	-58	56	5.46	102	B.A. 7	Precuneus	Parietal
2	54	40	5.44	48	N/A	N/A	N/A
-28	22	-16	5.40	18	B.A. 47	Inferior Frontal Gyrus	Frontal
-34	26	-4	5.32	10	B.A. 47	Inferior Frontal Gyrus	Frontal
-8	-78	-30	5.31	17	N/A	Declive	Cerebellum
-46	20	-24	5.25	27	B.A. 38	Superior Temporal Gyrus	Temporal
4	-44	32	5.19	59	B.A. 31	Cingulate Gyrus	Limbic
48	-26	-26	5.02	20	B.A. 20	Fusiform Gyrus	Temporal
-26	34	-24	5.00	23	B.A. 11	Inferior Frontal Gyrus	Frontal
-6	34	-30	4.94	10	B.A. 11	Orbital Gyrus	Frontal
24	12	58	4.91	33	B.A. 6	Middle Frontal Gyrus	Frontal
12	2	-8	4.86	17	Medial Globus Pallidus	Lentiform Nucleus	Sub-lobar
6	-34	-44	4.83	11	N/A	N/A	Medulla
4	32	34	4.80	21	B.A. 9	Medial Frontal Gyrus	Frontal
-8	-88	-34	4.77	9	N/A	Pyramis	Cerebellum
6	20	54	4.67	75	B.A. 8	Superior Frontal Gyrus	Frontal
22	20	32	4.60	12	N/A	Sub-Gyral	Frontal
16	-84	-24	4.52	9	N/A	Declive	Cerebellum
18	-4	-20	4.50	30	Amygdala	Parahippocampal Gyrus	Limbic
48	8	-40	4.40	10	B.A. 21	Middle Temporal Gyrus	Temporal
30	22	-22	4.39	9	N/A	Inferior Frontal Gyrus	Frontal
-40	-24	-16	4.20	6	B.A. 36	Parahippocampal Gyrus	Limbic
-26	-94	-22	4.20	8	B.A. 18	Fusiform Gyrus	Occipital
2	40	52	4.14	6	N/A	Superior Frontal Gyrus	Frontal
-12	26	30	4.13	7	B.A. 32	Cingulate Gyrus	Limbic
-64	-24	0	-9.91	3220	B.A. 22	Superior Temporal Gyrus	Temporal
62	-8	4	-9.87	3445	B.A. 22	Superior Temporal Gyrus	Temporal
50	-18	50	-8.30	208	B.A. 3	Postcentral Gyrus	Parietal
-30	-42	70	-6.52	39	N/A	Postcentral Gyrus	Parietal
24	-32	68	-6.51	206	B.A. 3	Postcentral Gyrus	Parietal
10	6	42	-6.09	263	B.A. 32	Cingulate Gyrus	Limbic
-16	-32	66	-6.00	76	B.A. 4	Precentral Gyrus	Frontal
12	18	-10	-5.08	35	B.A. 25	Anterior Cingulate	Limbic
10	32	-10	-5.06	21	B.A. 32	Anterior Cingulate	Limbic
34	-30	48	-5.01	26	B.A. 4	Precentral Gyrus	Frontal
18	-26	52	-4.81	7	B.A. 4	Precentral Gyrus	Frontal
-46	-48	42	-4.79	59	B.A. 40	Inferior Parietal Lobule	Parietal
-12	-24	76	-4.75	17	B.A. 6	Precentral Gyrus	Frontal
46	-36	60	-4.73	73	B.A. 40	Inferior Parietal Lobule	Parietal
26	10	0	-4.64	24	Putamen	Lentiform Nucleus	Sub-lobar
-16	24	-4	-4.63	6	Caudate Head	Caudate	Sub-lobar
-66	-52	32	-4.44	15	N/A	N/A	N/A
-66	-2	32	-4.43	22	N/A	N/A	N/A

-58	-8	46	-4.37	45	N/A	Precentral Gyrus	Frontal
28	50	-16	-4.12	6	B.A. 11	Superior Frontal Gyrus	Frontal

c.

X	Y	Z	BSR	Cluster Size	B.A.	Region	Lobe
38	-84	12	14.55	18041	B.A. 19	Middle Occipital Gyrus	Occipital
34	26	-10	11.46	1402	B.A. 47	Inferior Frontal Gyrus	Frontal
-42	-74	10	10.83	359	B.A. 39	Middle Temporal Gyrus	Temporal
-30	24	-14	10.08	559	B.A. 47	Inferior Frontal Gyrus	Frontal
-30	-2	50	9.37	1136	B.A. 6	Middle Frontal Gyrus	Frontal
36	2	46	8.32	1246	B.A. 6	Middle Frontal Gyrus	Frontal
2	52	40	8.25	1253	N/A	N/A	N/A
-26	-58	52	5.77	222	B.A. 7	Precuneus	Parietal
6	-78	-40	5.67	10	N/A	Pyramis	Cerebellum
-38	-20	-32	5.51	7	B.A. 20	Fusiform Gyrus	Temporal
-4	-56	-48	5.47	29	N/A	Cerebellar Tonsil	Cerebellum
-18	-88	-40	5.34	9	N/A	Tuber	Cerebellum
-40	-8	-28	5.32	22	B.A. 20	Fusiform Gyrus	Temporal
-54	-8	-16	5.09	9	B.A. 21	Middle Temporal Gyrus	Temporal
-10	26	28	5.08	48	B.A. 32	Anterior Cingulate	Limbic
18	-74	54	4.94	94	B.A. 7	Superior Parietal Lobule	Parietal
4	4	-14	4.88	16	N/A	Subcallosal Gyrus	Frontal
58	-14	-26	4.69	9	B.A. 20	Fusiform Gyrus	Temporal
50	-10	-16	4.64	8	B.A. 21	Middle Temporal Gyrus	Temporal
-20	-76	-48	4.62	10	N/A	Inferior Semi-Lunar Lobule	Cerebellum
6	16	26	4.62	17	B.A. 24	Anterior Cingulate	Limbic
-2	-68	-8	4.55	7	N/A	Culmen	Cerebellum
30	-58	50	4.55	47	B.A. 7	Superior Parietal Lobule	Parietal
-58	40	0	4.51	7	N/A	N/A	N/A
-8	-88	-34	4.47	11	N/A	Pyramis	Cerebellum
-44	-78	-36	4.47	6	N/A	Tuber	Cerebellum
-52	16	-26	4.37	17	B.A. 38	Superior Temporal Gyrus	Temporal
22	24	-18	4.35	9	B.A. 47	Inferior Frontal Gyrus	Frontal
8	32	32	4.29	33	B.A. 32	Cingulate Gyrus	Limbic
58	-6	2	-11.08	5598	B.A. 22	Superior Temporal Gyrus	Temporal
-46	-10	20	-9.89	5144	B.A. 43	Postcentral Gyrus	Parietal
-28	-42	64	-9.41	3865	B.A. 5	Postcentral Gyrus	Parietal

30	-42	68	-9.14	345	B.A. 5	Postcentral Gyrus	Parietal
12	38	-10	-5.78	33	B.A. 10	Medial Frontal Gyrus	Frontal
34	50	-8	-4.83	18	B.A. 11	Middle Frontal Gyrus	Frontal
-48	2	-14	-4.65	12	B.A. 38	Superior Temporal Gyrus	Temporal
-66	-52	34	-4.57	9	N/A	N/A	N/A
10	24	-6	-4.30	6	B.A. 24	Anterior Cingulate	Limbic
-42	-50	38	-4.16	13	B.A. 40	Inferior Parietal Lobule	Parietal

It was hypothesized that a latent variable that distinguished between the decrease negative and look negative conditions would also reach statistical significance. The second latent variable showed the predicted pattern, but it did not reach statistical significance ($p = 0.200$, Figure 8).

Figure 8. Experimental task condition weightings on LV2 for Task PLS. Conditions are depicted in the following order: look neutral (blue) look negative (red) decrease negative (green).

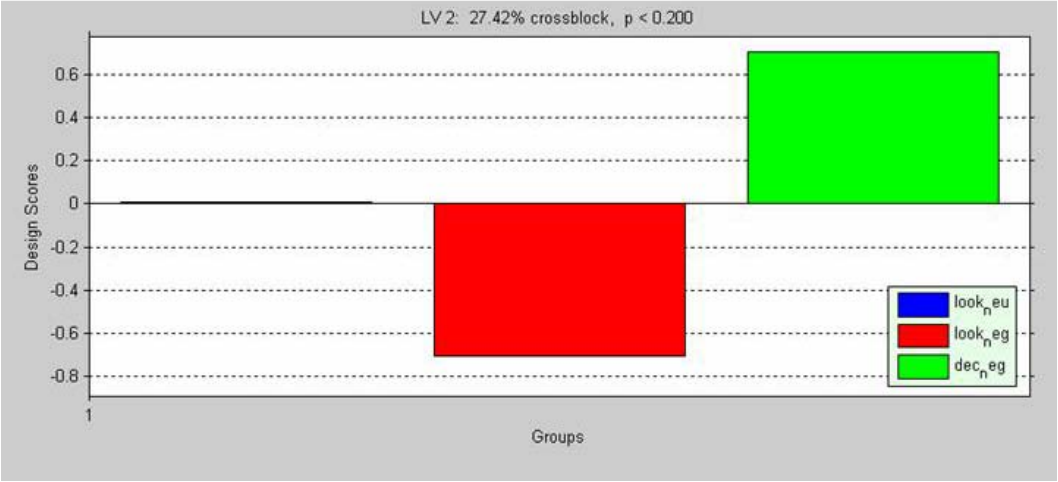

Next, values from the peak voxel in the right amygdala in LV1 were extracted for each non-zero lag (TRs 2, 3 and 4 of the picture-viewing period). These values were averaged across these time points to improve stability and entered into a seed PLS to identify regions that significantly vary with amygdala activity. Significant clusters from this seed PLS can be found in Table 5 and Figure 9.

Figure 9. LV1 for right amygdala PLS, Study 1, displayed over normalized T1-weighted anatomical image. Lags (TRs) 0-4 are depicted in the descending rows. Cool colors represent positive covariation with the right amygdala seed voxel.

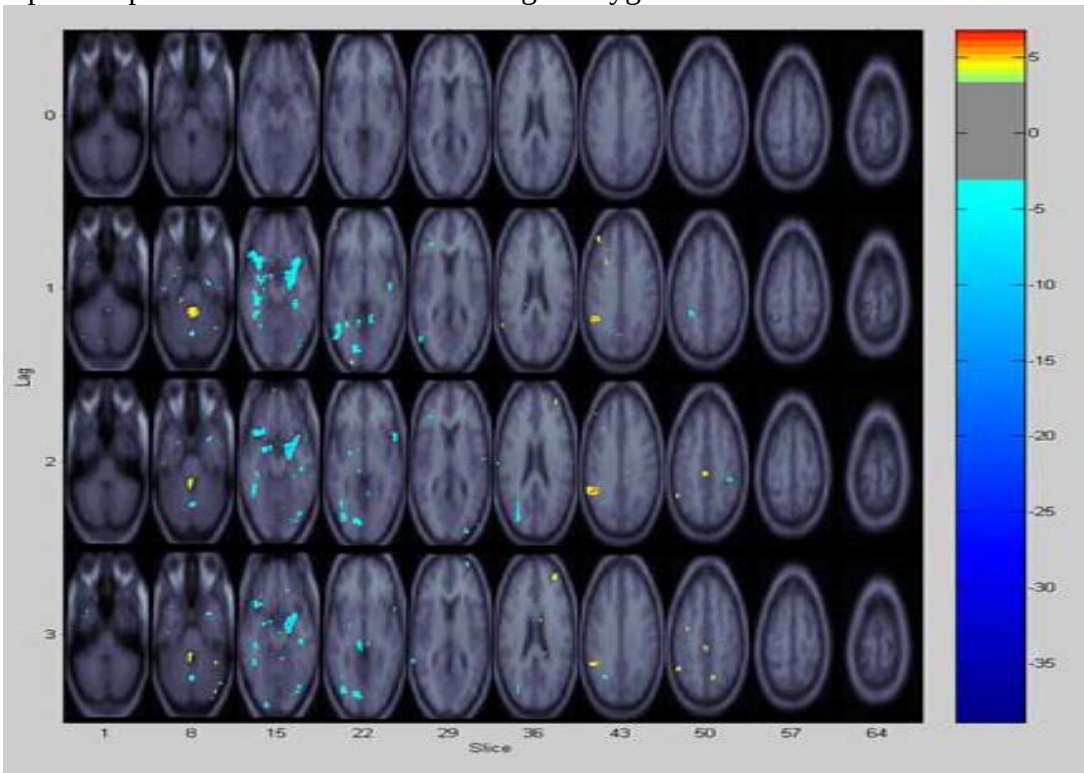

Table 5. Clusters with p<0.0001 from LV1, right amygdala seed PLS. XYZ values represent MNI coordinates. B.A. = Brodmann Area. BSR= bootsrap ratio. Region labels from Talairach Daemon. a. Lag 1 b. Lag 2 c. Lag 3.

a.

X	Y	Z	BSR	Appro.P	Cluster Size	B.A.	Region	Lobe
-28	12	38	6.83	<0.0001	40	B.A. 8	Middle Frontal Gyrus	Frontal
-52	-82	-26	5.90	<0.0001	54	N/A	Declive	Cerebellum
38	-26	0	5.55	<0.0001	45	N/A	Claustrum	Sub-lobar
-46	-50	36	5.34	<0.0001	152	B.A. 40	Inferior Parietal Lobule	Parietal
8	-42	-34	5.13	<0.0001	131	N/A	N/A	Cerebellum
-2	-28	44	5.12	<0.0001	17	N/A	Cingulate Gyrus	Limbic
2	28	4	5.11	<0.0001	7	N/A	Anterior Cingulate	Limbic
-42	34	44	4.70	<0.0001	69	B.A. 8	Middle Frontal Gyrus	Frontal
-16	32	-4	4.39	<0.0001	6	B.A. 10	Medial Frontal Gyrus	Frontal
18	56	-4	4.21	<0.0001	6	B.A. 10	Superior Frontal Gyrus	Frontal
-4	-68	38	4.16	<0.0001	27	B.A. 7	Precuneus	Parietal
-22	-98	-8	4.10	<0.0001	12	B.A. 18	Cuneus	Occipital
20	30	26	3.88	1E-04	8	B.A. 32	Anterior Cingulate	Limbic
-20	-30	-36	3.85	1E-04	7	N/A	N/A	Pons
-62	-60	24	3.71	2E-04	13	B.A. 39	Superior Temporal Gyrus	Temporal
-26	26	34	3.57	4E-04	7	B.A. 9	Middle Frontal Gyrus	Frontal
20	-6	-18	-16.81	<0.0001	1046	Amygdala	Parahippocampal Gyrus	Limbic
32	-34	-28	-6.91	<0.0001	53	N/A	Culmen	Cerebellum
2	12	22	-6.89	<0.0001	55	B.A. 33	Anterior Cingulate	Limbic
-44	22	-28	-6.47	<0.0001	606	B.A. 38	Superior Temporal Gyrus	Temporal
2	-14	-26	-6.38	<0.0001	33	N/A	N/A	Pons
-42	-22	-24	-6.34	<0.0001	257	B.A. 36	Parahippocampal Gyrus	Limbic
-52	-78	-4	-6.07	<0.0001	379	N/A	Middle Occipital Gyrus	Occipital
-2	-8	0	-5.90	<0.0001	59	N/A	Third Ventricle	Sub-lobar
48	-12	-12	-5.78	<0.0001	98	B.A. 21	Sub-Gyral	Temporal
14	-46	-14	-5.55	<0.0001	140	N/A	Culmen	Cerebellum
44	30	2	-5.55	<0.0001	28	B.A. 45	Inferior Frontal Gyrus	Frontal
0	-64	-40	-5.30	<0.0001	38	N/A	Uvula	Cerebellum
-14	-84	-10	-5.05	<0.0001	171	B.A. 18	Lingual Gyrus	Occipital
-10	-2	42	-4.86	<0.0001	32	B.A. 24	Cingulate Gyrus	Limbic

				<0.0001			Inferior Temporal	
-40	-2	-42	-4.79		19	B.A. 20	Gyrus	Temporal
-30	-44	48	-4.66	<0.0001	108	N/A	Sub-Gyral	Parietal
-12	18	-14	-4.56	<0.0001	6	B.A. 47	Subcallosal Gyrus	Frontal
				<0.0001			Superior Temporal	
62	12	-16	-4.47		11	N/A	Gyrus	Temporal
				<0.0001				
-10	-54	-8	-4.45		19	N/A	Culmen	Cerebellum
				<0.0001			Parahippocampal	
-24	-18	-18	-4.45		44	B.A. 28	Gyrus	Limbic
				<0.0001				
-50	-50	-28	-4.44		16	N/A	Declive	Cerebellum
40	-12	-28	-4.30	<0.0001	6	B.A. 20	Fusiform Gyrus	Temporal
56	8	14	-4.24	<0.0001	8	B.A. 44	Inferior Frontal Gyrus	Frontal
-36	-62	-4	-4.17	<0.0001	10	N/A	Sub-Gyral	Occipital
10	20	44	-4.13	<0.0001	20	B.A. 32	Cingulate Gyrus	Limbic
40	-78	-20	-4.12	<0.0001	20	B.A. 19	Fusiform Gyrus	Occipital
4	-78	-42	-4.05	1E-04	7	N/A	N/A	N/A
							Parahippocampal	
-30	-56	-10	-4.02	1E-04	22	B.A. 19	Gyrus	Limbic
24	-86	-18	-3.94	1E-04	10	B.A. 19	Fusiform Gyrus	Occipital
-2	24	-24	-3.93	1E-04	6	B.A. 11	Rectal Gyrus	Frontal
-32	32	12	-3.92	1E-04	23	B.A. 46	Inferior Frontal Gyrus	Frontal
-22	-2	54	-3.77	2E-04	9	B.A. 6	Sub-Gyral	Frontal
10	-92	-4	-3.73	2E-04	7	B.A. 17	Lingual Gyrus	Occipital
							Inferior Occipital	
-32	-78	-6	-3.71	2E-04	8	B.A. 19	Gyrus	Occipital
40	2	32	-3.70	2E-04	11	N/A	Precentral Gyrus	Frontal
							Middle Occipital	
30	-88	6	-3.64	3E-04	7	B.A. 19	Gyrus	Occipital
32	2	54	-3.49	5E-04	13	B.A. 6	Middle Frontal Gyrus	Frontal

b.

X	Y	Z	BSR	Appro.P	Cluster Size	B.A.	Region	Lobe
-54	-48	32	6.79	<0.0001	221	B.A. 40	Supramarginal Gyrus	Parietal
-4	-32	46	5.61	<0.0001	94	B.A. 31	Paracentral Lobule	Frontal
-4	-38	-36	4.99	<0.0001	96	N/A	N/A	Pons
36	44	12	4.52	<0.0001	44	B.A. 10	Middle Frontal Gyrus	Frontal
				<0.0001				
50	-70	-34	4.15		13	N/A	Tuber	Cerebellum
				<0.0001				
36	-88	-40	4.09		9	N/A	Tuber	Cerebellum
26	44	42	3.89	0.0001	6	N/A	Superior Frontal Gyrus	Frontal
-44	36	36	3.82	0.0001	10	B.A. 9	Superior Frontal Gyrus	Frontal
38	50	22	3.78	0.0002	17	B.A. 10	Middle Frontal Gyrus	Frontal
16	58	-26	3.73	0.0002	11	B.A. 11	Superior Frontal Gyrus	Frontal

20	-4	-18	-24.25	<0.0001	655	Amygdala	Parahippocampal Gyrus	Limbic
-36	-8	-42	-9.01	<0.0001	73	B.A. 20	Inferior Temporal Gyrus	Temporal
4	10	24	-7.22	<0.0001	46	B.A. 33	Anterior Cingulate	Limbic
-34	16	-22	-7.17	<0.0001	167	N/A	Superior Temporal Gyrus	Temporal
-14	-80	-14	-7.16	<0.0001	185	B.A. 18	Lingual Gyrus	Occipital
-24	-4	-20	-6.10	<0.0001	107	Amygdala	Parahippocampal Gyrus	Limbic
-46	-52	-26	-6.04	<0.0001	82	N/A	Culmen	Cerebellum
2	-64	-40	-6.01	<0.0001	43	N/A	Uvula	Cerebellum
-36	-76	-6	-5.58	<0.0001	112	B.A. 19	Inferior Occipital Gyrus	Occipital
-30	-74	16	-5.37	<0.0001	128	N/A	Middle Temporal Gyrus	Temporal
4	-16	-28	-5.30	<0.0001	24	N/A	N/A	Pons
52	-86	2	-5.19	<0.0001	13	B.A. 19	Middle Occipital Gyrus	Occipital
50	14	14	-4.99	<0.0001	32	B.A. 44	Inferior Frontal Gyrus	Frontal
68	-44	4	-4.91	<0.0001	18	B.A. 22	Superior Temporal Gyrus	Temporal
-42	-24	-30	-4.65	<0.0001	61	B.A. 20	Fusiform Gyrus	Temporal
-26	-26	-12	-4.64	<0.0001	10	Hippocampus	Sub-Gyral	Temporal
-2	12	-4	-4.62	<0.0001	10	B.A. 25	Anterior Cingulate	Limbic
-16	30	-24	-4.56	<0.0001	10	B.A. 11	Inferior Frontal Gyrus	Frontal
42	-74	-22	-4.36	<0.0001	89	N/A	Declive	Cerebellum
8	-54	-6	-4.34	<0.0001	20	N/A	Culmen	Cerebellum
-66	-42	12	-4.33	<0.0001	17	B.A. 22	Superior Temporal Gyrus	Temporal
42	-36	48	-4.27	<0.0001	23	B.A. 40	Inferior Parietal Lobule	Parietal
54	14	-10	-4.27	<0.0001	57	B.A. 38	Superior Temporal Gyrus	Temporal
10	-4	32	-4.09	<0.0001	22	B.A. 24	Cingulate Gyrus	Limbic
-10	34	44	-4.02	0.0001	30	B.A. 8	Medial Frontal Gyrus	Frontal
-10	-4	-10	-3.97	0.0001	6	Hypothalamus	N/A	Sub-lobar
-62	-24	38	-3.95	0.0001	15	B.A. 1	Postcentral Gyrus	Parietal
-32	26	-2	-3.93	0.0001	6	B.A. 47	Inferior Frontal Gyrus	Frontal
30	-92	6	-3.91	0.0001	21	B.A. 19	Middle Occipital Gyrus	Occipital
64	-16	8	-3.90	0.0001	7	B.A. 42	Transverse Temporal Gyrus	Temporal
6	24	40	-3.90	0.0001	10	B.A. 32	Cingulate Gyrus	Frontal
-48	22	-30	-3.79	0.0001	8	N/A	N/A	N/A
-34	30	10	-3.79	0.0001	20	B.A. 45	Inferior Frontal Gyrus	Frontal

44	-26	-22	-3.73	0.0002	7	B.A. 20	Fusiform Gyrus	Temporal
58	-6	-14	-3.71	0.0002	15	B.A. 21	Inferior Temporal Gyrus	Temporal
-10	-26	-6	-3.70	0.0002	8	N/A	N/A	Midbrain
30	28	-16	-3.64	0.0003	11	B.A. 47	Inferior Frontal Gyrus	Frontal

c.

X	Y	Z	BSR	Appro.P	Cluster Size	B.A.	Region	Lobe
-44	-48	36	5.88	<0.0001	75	B.A. 40	Supramarginal Gyrus	Parietal
30	38	10	5.03	<0.0001	101	N/A	Sub-Gyral	Frontal
-4	-40	-34	4.86	<0.0001	86	N/A	N/A	Cerebellum
-52	-54	52	4.77	<0.0001	32	N/A	Inferior Parietal Lobule	N/A
10	2	22	4.71	<0.0001	11	N/A	Lateral Ventricle	Sub-lobar
-56	-20	-12	4.65	<0.0001	16	B.A. 21	Middle Temporal Gyrus	Temporal
10	-64	50	4.48	<0.0001	41	N/A	Precuneus	Parietal
-6	-52	54	4.28	<0.0001	24	B.A. 7	Precuneus	Parietal
-4	-28	42	4.07	<0.0001	49	B.A. 31	Cingulate Gyrus	Limbic
44	-48	-36	3.84	0.0001	6	N/A	Culmen	Cerebellum
44	-80	-36	3.80	0.0001	7	N/A	Tuber	Cerebellum
-36	-10	48	3.65	0.0003	8	B.A. 6	Middle Frontal Gyrus	Frontal
24	-86	-2	3.58	0.0003	6	B.A. 18	Middle Occipital Gyrus	Occipital
22	-6	-18	-38.89	<0.0001	557	Amygdala	Parahippocampal Gyrus	Limbic
-38	-6	-42	-6.24	<0.0001	30	B.A. 20	Inferior Temporal Gyrus	Temporal
-14	-80	-14	-6.17	<0.0001	162	B.A. 18	Lingual Gyrus	Occipital
32	2	-46	-5.80	<0.0001	57	B.A. 20	Inferior Temporal Gyrus	Temporal
-46	-52	-26	-5.80	<0.0001	61	N/A	Culmen	Cerebellum
40	-24	-22	-5.53	<0.0001	23	B.A. 36	Parahippocampal Gyrus	Limbic
-40	16	-24	-5.25	<0.0001	112	B.A. 38	Superior Temporal Gyrus	Temporal
-8	-28	-8	-5.20	<0.0001	61	N/A	N/A	Midbrain
2	-8	0	-5.19	<0.0001	33	N/A	Thalamus	Sub-lobar
38	-76	-22	-5.14	<0.0001	62	N/A	Declive	Cerebellum
-24	-4	-18	-5.13	<0.0001	87	Amygdala	Parahippocampal Gyrus	Limbic
20	-34	-12	-5.08	<0.0001	52	B.A. 35	Parahippocampal Gyrus	Limbic

				<0.0001			Inferior Occipital	
-34	-76	-6	-4.79		66	B.A. 19	Gyrus	Occipital
46	14	16	-4.78	<0.0001	14	B.A. 44	Inferior Frontal Gyrus	Frontal
				<0.0001				
0	-64	-36	-4.70		35	N/A	Uvula	Cerebellum
-4	14	22	-4.63	<0.0001	28	B.A. 33	Anterior Cingulate	Limbic
				<0.0001			Middle Occipital	
52	-86	2	-4.58		8	B.A. 19	Gyrus	Occipital
-42	-26	-26	-4.54	<0.0001	58	B.A. 20	Fusiform Gyrus	Temporal
8	-28	-8	-4.50	<0.0001	6	N/A	N/A	Midbrain
2	-14	-24	-4.44	<0.0001	26	N/A	N/A	Pons
-22	-94	-24	-4.36	<0.0001	15	B.A. 18	Fusiform Gyrus	Occipital
-70	-44	10	-4.30	<0.0001	32	N/A	N/A	N/A
				<0.0001				
6	-42	-22	-4.24		10	N/A	Culmen	Cerebellum
-14	28	-28	-4.23	<0.0001	14	B.A. 47	Orbital Gyrus	Frontal
				<0.0001			Inferior Temporal	
-44	-14	-34	-4.23		8	B.A. 20	Gyrus	Temporal
34	60	6	-4.16	<0.0001	17	B.A. 10	Middle Frontal Gyrus	Frontal
							Middle Temporal	
-32	-74	16	-4.05	0.0001	40	N/A	Gyrus	Temporal
							Inferior Temporal	
42	-10	-34	-3.95	0.0001	8	B.A. 20	Gyrus	Temporal
							Middle Temporal	
-40	-64	-6	-3.85	0.0001	13	B.A. 37	Gyrus	Occipital
-30	-62	34	-3.83	0.0001	19	B.A. 39	Angular Gyrus	Parietal
							Inferior Parietal	
40	-40	44	-3.75	0.0002	8	B.A. 40	Lobule	Parietal

Selection of regions

Significant clusters identified in the right amygdala seed PLS were selected for inclusion in the SEM based on several criteria. Regions were selected if the same anatomical regions were also identified in an independent right amygdala seed PLS performed upon a separate sample of men and women (N= 44). This previous study was of negative and neutral picture perception presented in a block design using positron emission tomography (PET) imaging. Details of this study can be found in Appendix A. In addition, the regions included have been identified in the previous literature as involved in the processing of negative emotional information. It is notable that because

the present study focused upon the interaction between emotion-responsive regions and prefrontal cortex, several regions that are known to be influenced by emotional stimuli were not included in the model (i.e., visual cortex, brainstem, thalamus, cerebellum). A list of regions chosen for inclusion is shown in Table 6.

Table 6. Peak voxels used in SEM. B.A. = Brodmann Area. BSR= bootsrap ratio. Region labels from Talairach Daemon.

X	Y	Z	BSR	Appro.P	Cluster Size	B.A.	Region	Lobe
2	12	22	-6.89	<0.0001	117	B.A. 33	Anterior Cingulate	Limbic
30	38	10	5.029	<0.0001	301	N/A	Inferior Frontal Gyrus	Frontal
10	-64	50	4.481	<0.0001	115	N/A	Precuneus	Parietal
30	50	42	3.824	0.0001	33	B.A. 9	Superior Frontal Gyrus	Frontal
22	-6	-18	-38.9	<0.0001	1086	Amygdala	Parahippocampal Gyrus	Limbic
-2	10	-4	-3.2	0.0014	18	B.A. 25	Anterior Cingulate	Limbic
36	16	4	-3.17	0.0015	14	N/A	Insula	Sub-lobar

SEM

The correlation matrices derived from the seed PLS analyses were used to compare relative model fit between conditions. The stacked model in LISREL indicated better model fit when paths were free to differ between the look negative and look neutral conditions (χ^2_{diff} (28)= 42.37, p<0.04). Testing each path individually indicated that 5 paths significantly affected differential model fit. The models for the look negative and look neutral conditions can be found in Figure 10. The paths that differ significantly between the negative and neutral conditions can be found in Table 7. Final differential model fit was significant (χ^2_{diff} (5)= 25.24, p<0.0001). The reciprocal paths between

SFG and sACC were more negative during the look negative than the look neutral condition. The reciprocal paths between inferior frontal gyrus and ACC were more positive during the negative than the neural condition. Lastly, the path from precuneus to sACC was more negative during the negative than the neutral condition.

Table 7. Paths from SEM. Paths listed contributed significantly to the difference in χ^2 between look negative and look neutral conditions. Coordinates for regions are listed in Table 3. sACC = subgenual anterior cingulate cortex, SFG= superior frontal gyrus, ACC= anterior cingulate cortex, IFG= inferior frontal gyrus.

from	to	χ^2	negative	neutral
SFG	sACC	6.36	-0.19	0.18
IFG	rACC	12.8	0.44	-0.21
rACC	IFG	7.16	0.14	-0.07
sACC	SFG	4.81	-0.06	0.21
precuneus	sACC	3.91	-0.07	0.36

Figure 10. SEM. Lines in red indicate paths that differ significantly between the look negative and look neutral conditions.

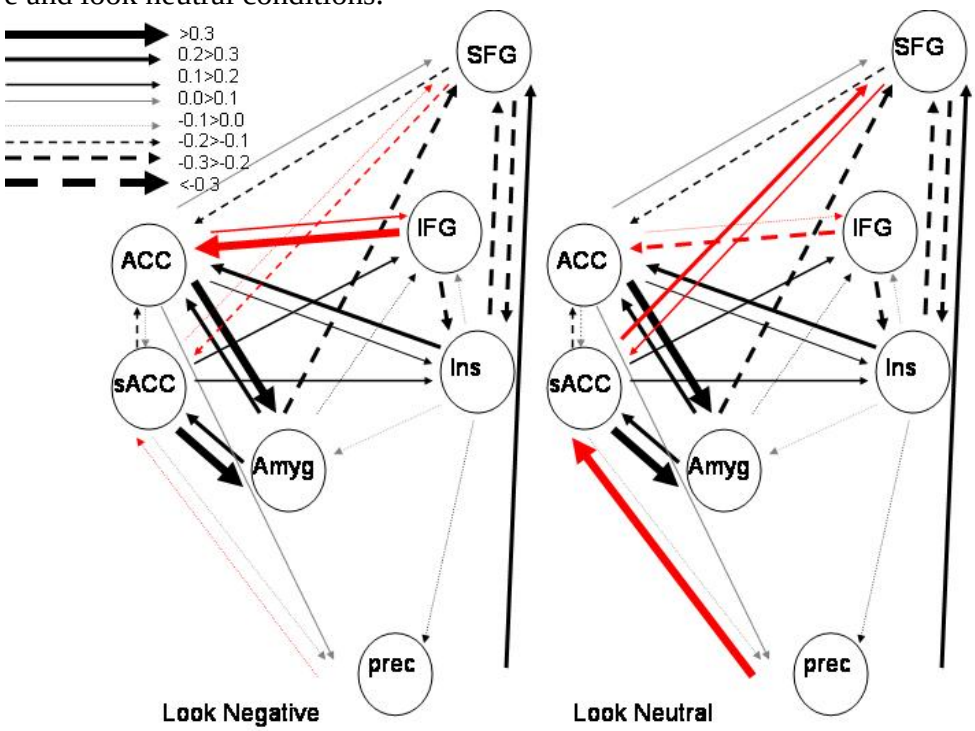

A separate stacked model in LISREL did not strongly indicate better model fit when paths were free to differ between the look negative and decrease negative conditions(χ^2_{diff} (28)= 35.67, p=0.15). However, because this was the a priori comparison of interest, individual paths were tested. Testing each path individually indicated that 3 paths significantly affected differential model fit. Comparisons of the look negative and decrease negative conditions can be found in Figure 11. Final differential model fit was significant (χ^2_{diff} (3) = 14.73, p<0.002). The paths that differ significantly between the decrease negative and look negative conditions can be found in Table 8.

Figure 11. SEM. Lines in red indicate paths that differ significantly between the decrease negative and look negative conditions.

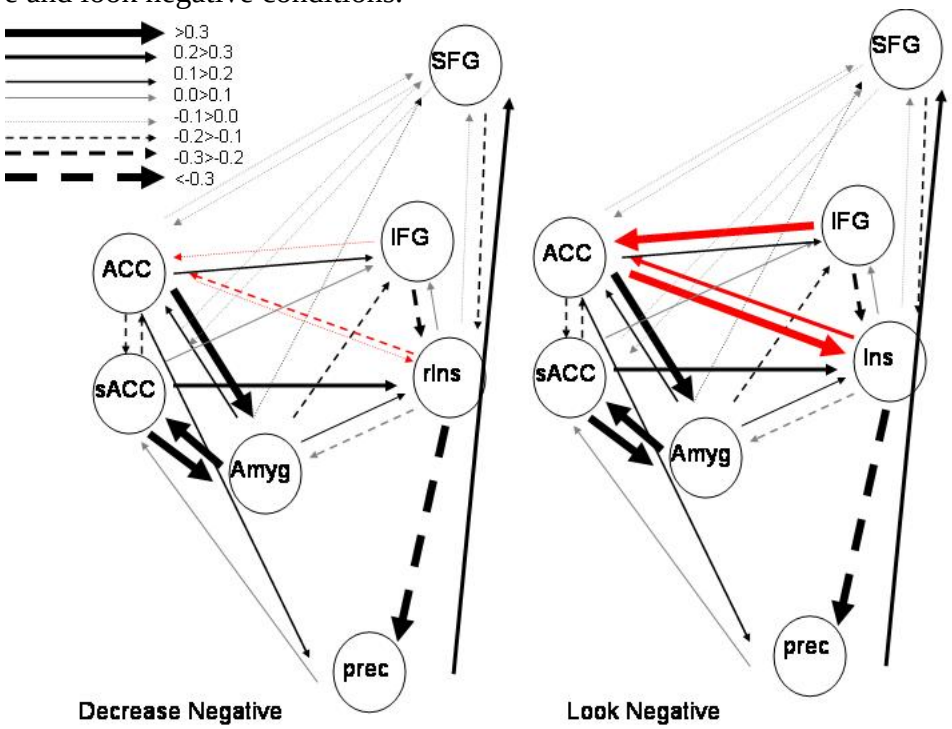

Table 8. Paths from SEM. Paths listed contributed significantly to the difference in χ^2 between decrease negative and look negative conditions. Coordinates for regions are listed in Table 3. ACC= anterior cingulate cortex, IFG= inferior frontal gyrus.

from	to	χ^2	df	decrease	look
insula	ACC	6.94	1	-0.12	0.24
IFG	ACC	5.32	1	-0.01	0.51
ACC	insula	7.96	1	-0.08	0.3

The regions for which effective connectivity differed were IFG, ACC, and insula. The path from IFG to ACC was less positive during decrease negative than look negative. In addition, the reciprocal paths from ACC to insula were more negative during decrease negative than look negative. Because there was a strong positive path from ACC to amygdala, the net effect of the change in the path from IFG to ACC was a reduction in the positive influence on the amygdala. Similarly, although the path from ACC to insula changed sign between the conditions, the overall influence of IFG on insula through the ACC was half as strong during the decrease negative than the look negative condition.

DISCUSSION

Summary of results

The PLS analysis revealed one LV that significantly explained the covariance in the brain-task block. This LV distinguished between both negative conditions (look negative and decrease negative) and the look neutral condition. This LV identified several regions that are typically active during emotional processing, including a small cluster in the right amygdala. The peak voxel from the right amygdala was chosen for the seed analysis. This seed analysis, along with the previous literature and a right amygdala seed PLS performed upon an independent sample, yielded seven regions that were entered into an SEM. The regions for which effective connectivity significantly differed between the look negative and look neutral conditions were the SFG, the IFG, the ACC, and the precuneus. The reciprocal paths between the IFG and the ACC were more strongly positive during the look negative than the look neutral condition, whereas the paths between the SFG and the sACC, and the path from the precuneus to the sACC were more strongly negative during the look negative than the look neutral condition. For the decrease negative vs. look negative comparison, the regions that differed in effective connectivity were the insula, the ACC, and the IFG. The path from IFG to ACC was less positive during decrease negative than look negative. In addition, the reciprocal paths from ACC to insula were more negative during decrease negative than look negative.

Multivariate vs. univariate results

Although it was hypothesized that another set of regions would be identified in the task PLS that distinguished between the look negative and decrease negative conditions, the second LV that showed this pattern did not reach statistical significance. In fact, the first LV, which distinguished between both negative conditions and the neutral condition, accounted for almost three-fourths of the covariance in the task PLS. This raises several points to consider. The first is that even though the regions identified in the basic SPM contrasts were similar to those found in other studies of the cognitive down-regulation of emotion, multivariate analyses revealed that most of the covariance in the data can be characterized by differences between the presentation of negative and neutral pictures. It is difficult to draw strong conclusions about the non-significance of the second LV, given the small number of conditions in the present study. However, the right amygdala seed PLS did not indicate that the relationship between any of the regions identified and the amygdala significantly differed between conditions, which also indicates that the differences between conditions should be interpreted with caution. Lastly, it is notable that the first LV's weighting on the different conditions does not represent any typically performed a priori comparison (both negative conditions greater than neutral). Therefore, most neuroimaging studies of the cognitive regulation of emotion do not perform the comparison that might explain the largest portion of the variance in their data. In this case, the differences between the regulation and non-regulation conditions were dwarfed by differences between the negative and neutral stimuli. As more and more studies interpret the differences between increasingly similar

cognitive tasks performed upon emotional stimuli, this is an important reminder of the relative magnitude of stimulus-driven emotional responding.

Regions implicated in effective connectivity of emotion regulation

The crucial regions that differ in effective connectivity between the regulation and non-regulation conditions are the insula, the ACC, and the IFG. The IFG has been identified as consistently involved in cognitive control (Amunts & von Cramon, 2006), most notably during inhibition tasks (Garavan, Hester, Murphy, Fassbender, & Kelly, 2006; Ray Li, Huang, Constable, & Sinha, 2006; Rubia et al., 2003). In addition, activation of this region has been reported during tasks that involve the cognitive processing of emotional stimuli, which may have a regulatory effect (Hariri, Bookheimer, & Mazziotta, 2000; Taylor, Eisenberger, Saxbe, Lehman, & Lieberman, 2006).

The ACC is most typically conceptualized as more active during conflict detection and attention monitoring and has recently been hypothesized to actively recruit lateral prefrontal regions when control is needed (Amunts & von Cramon, 2006; Kerns et al., 2004). The particular subregion of the ACC included in this study is the dorsal ACC, which at one point was conceptualized as the relatively "cognitive" division of the ACC (Bush et al., 2000; Devinsky, Morrell, & Vogt, 1995). However, several recent reports indicate that this region is involved in the interaction between emotion and cognition (Elliot et al., 2000), attentional manipulations performed upon emotional experience (Hutcherson et al., 2005) and individual differences related to emotional awareness (Lane et al., 1998; McRae, Reiman, Fort, Chen, & Lane, under review) and emotion regulation

(Ochsner et al., 2002). Given these varied roles in emotional and cognitive processing, the ACC is well-positioned (theoretically and anatomically) to interface between cognitive control regions and emotion-responsive regions.

The insula has a documented role in the processing of several types of negative emotion, and is often thought to be primarily engaged during the experience of disgust (Critchley, Wiens, Rotshtein, Öhman, & Dolan, 2004; Lane, Reiman, Ahern, Schwartz, & Davidson, 1997; Phan et al., 2002; Phillips, Drevets, Rauch, & Lane, 2003; Sanfey, Rilling, Aronson, Nystrom, & Cohen, 2003; Vaitl et al., 2005). In particular, the insula is thought to be involved in the representation of one's subjective emotional experience and current visceral state (Critchley, Elliott, Mathias, & Dolan, 2000; Critchley et al., 2004).

Significantly different paths

The differences in effective connectivity between the decrease negative and look negative conditions can be interpreted on several levels. The most conservative approach is to strictly limit interpretations to the paths that differ between conditions. In this case, it would be inappropriate to interpret the differences in the path from IFG to ACC in relation to the path from ACC to amygdala (for example). It is noteworthy that only one path significantly distinguishes between look negative and look neutral as well as decrease negative and look negative conditions. That path (IFG to ACC) was significantly more positive during look negative than look neutral, and was significantly more positive during look negative than decrease negative. Therefore, one can conclude that if a stronger positive relationship between IFG and ACC characterizes the look

negative condition, the strength of that path is significantly diminished by the instruction to regulate. In addition, the path from ACC to insula also becomes more negative during the decrease negative condition compared to the look negative condition. This is also consistent with the notion that the influence of prefrontal regions upon emotion-responsive regions becomes significantly less positive during emotion regulation. However, it is encouraging that the nature of the other paths in the model (that do not significantly differ between conditions) is in line with current conceptualizations of emotion regulation. Namely, the paths that distinguish between look negative and decrease negative imply a significant diminution of the positive influence of cognitive control areas over other emotion-related areas (amygdala).

Implications

The present study makes several contributions to the understanding of the down-regulation of negative emotion. First, the results presented here support the common interpretation of previous findings from subtraction-based contrasts and measures of functional connectivity. More specifically, the SEMs in the present study are consistent with the assertion that prefrontal regions exert an inhibitory influence upon emotion-responsive regions during emotion regulation.

The present study reports the modulation of three paths when participants are engaging in effortful emotion regulation. The path from IFC to ACC, as well as the reciprocal paths between ACC and insula, are significantly less positive (or more negative) during the regulation trials than the non-regulation trials. The evidence

reviewed above indicates that the IFG plays a role in the implementation of cognitive control and working memory, the ACC is involved in direction attention towards emotion, and that activity in the insula relates to the subjective experience of emotion. Given these respective roles, I propose that changes in effective connectivity during emotion regulation represent two types of processing, one represented by the change from IFG to ACC, and one represented by the ACC-insula loop. These two processes are described below. Future studies that would directly test hypotheses generated by this two-process model are proposed, and implications for clinical models of emotion dysregulation are discussed.

Two main changes in effective connectivity were observed: a change in the IFG-ACC path, and a change in the reciprocal paths between ACC and insula. Given that the IFG has a documented role in working memory (Tsukiura et al., 2001), updating relevant task instructions (Brass & Cramon, 2004), and implementing inhibitory control (Aron, Fletcher, Bullmore, Sahakian, & Robbins, 2003), it is not unlikely that the paths from the IFG are heavily involved in maintaining task instructions and facilitating processes that are consistent with task instructions. The ACC has a documented role in directing attention towards emotion. The “look” instruction emphasized allowing oneself to respond naturally to the emotional nature of the stimuli and to attend to any feeling that might be elicited. Therefore, the emotional aspects of the stimuli, as well as the strength of one’s own negative affect, are more closely related to task-specific goals in the look negative than the decrease negative instruction. Therefore, the more positive path from

IFG to ACC in the look negative condition may reflect the facilitation of attention towards emotion in accordance with task goals.

"Attention towards emotion," could refer to several types of processing. Attention can be directed towards the emotional aspects of external stimuli, or towards one's subjective emotional state. The dorsal region of the ACC included in the present model has been implicated in several types of attentional control. In particular, the ACC appears to be engaged when individuals are asked to focus their attention upon their current emotional experience (Hutcherson et al., 2005; Taylor, Phan, Decker, & Liberzon, 2003), as well as when individuals are asked to focus their attention upon emotional aspects of the presented stimuli (Elliot et al., 2000). These attention-regulatory properties of the dACC may both play a role in the regulation of emotion, but they may have their effect on different emotion-responsive regions.

Two emotion-responsive regions receive input from the ACC in the present model: the amygdala and the insula. The path from the ACC to the insula is more negative when individuals are instructed to regulate. In addition, the reverse path from the insula to the ACC is significantly more negative during the regulated condition than the look condition. Previous reports have implicated the anterior insula in the representation of one's subjective emotional experience and current visceral state (Critchley et al., 2000; Critchley et al., 2004). It is plausible then, that the reciprocal paths between ACC and insula constitute a more positive feedback system during the unregulated condition and a more negative feedback system during the regulated condition. When one is currently feeling negative, and then focuses one's attention upon

that negative state, this is likely to amplify the negative affect in a way that is consistent with a positive feedback loop. However, if one is focusing less attention upon one's negative feeling, it is likely that the feeling will diminish in a fashion that is consistent with a negative feedback loop. These positive and negative feedback loops are plausible, considering the processing that is likely to occur during the unregulated and regulated negative conditions respectively.

No path that is directly afferent to the amygdala changes in value between the regulated and unregulated conditions. This may seem surprising given the regularity with which decreases in amygdala activity are reported in the literature, and the fact that the amygdala was the seed region chosen for the present analysis. However, the fact that these paths do not change by condition does not mean that the present model is inconsistent with a negative influence on amygdala from control-related regions. Because there is a strongly positive path from the ACC to the amygdala, it is likely that the more negative influence of IFG on ACC during regulation has the downstream consequence of decreased amygdala activity. However, unlike the insula, there is no reciprocal negative connection between the ACC and the amygdala.

The amygdala is often conceptualized as identifying and responding to features in the environment with probable emotional value (Hadjikhani & de Gelder, 2003; Whalen et al., 2004; Wright, Martis, Shin, Fischer, & Rauch, 2002). Unlike the insula, one might not expect this process to involve a reciprocally positive relationship with attentional regions like the ACC. If the amygdala responds to the emotionally salient features in a stimulus that are attended to, the response in the amygdala should be proportional to the

attention allocated towards those features. This is represented by the strongly positive path from ACC to amygdala. However, if less attention is allocated towards those features, as is proposed during the regulation condition, there is no reason to predict that a negative feedback loop would be in place as is the case for the insula. Rather, the substrate of interest for the amygdala, the emotional aspects of the external stimulus, is present to be processed as soon as attention is directed towards it. By contrast, the substrate of interest for the insula, the emotional aspect of one's subjective experience, is by definition more and more diminished the longer it is kept out of attentional focus.

The present interpretation of results generates several hypotheses for future studies to investigate. The first is that decreases in amygdala activity during cognitive regulation result from a decrease in attention towards the emotional characteristics in the stimuli. Therefore, studies that obtain eye-tracking data, or use a task such as the dot-probe to index attention towards different spatial locations, may indicate that amygdala activity is related to the degree to which emotional features of these complex scenes are given the advantage of attention. In addition, one might hypothesize that amygdala activity can most effectively be decreased if the emotion regulation instructions emphasize the diversion of attention from the emotional aspects of the stimulus.

Alternatively, the present interpretation of results might predict that emotion regulation strategies that more directly target subjective feeling would impact the insula response to these negative pictures. If subjects are allowed to modify their subjective state using imagery, memories, or by directly manipulating physiology, one might expect to see decreases in insula activity.

It should be noted that the present model focuses upon changes in effective connectivity during seconds 2-8 of the picture-viewing portion of the task. If the analysis instead focused upon the earliest time points in the picture-viewing task, or even the regulation instruction period, several of the regions of interest may be performing different functions.

The ACC has been implicated not just in the allocation of attention towards emotion, but also in conflict monitoring (Botvinick et al., 2004; Fassbender et al., 2004) and signaling the need for cognitive control (Amunts & von Cramon, 2006; Kerns et al., 2004). Therefore, one might expect to observe a more positive path from the ACC to the IFG during the regulation than the non-regulation condition. However, such a change was not observed in the present data set, and instead increased negativity in the IFG → ACC path was observed. Therefore, the present interpretation emphasizes the role of the ACC in actively allocating attention towards emotion in accordance with task-specific goals. However, the ACC may perform these different functions in different contexts, or during different time points in the regulation process. The proposed ACC to IFG change, reflecting its recruiting and monitoring function, might be observed during preparation for implementing the instruction. Later in the trial, the ACC may instead implement changes in attention allocation towards emotion as outlined above.

The proposed role for the amygdala indicates that amygdala activity is in part determined by the amount of attention allocated to the emotional features of the stimulus in accordance with task goals. However, this top-down account of amygdala activation is inconsistent with reports of amygdala activation that is not modulated by attention

(Anderson, Christoff, Panitz, De Rosa, & Gabrieli, 2003; Hutcherson et al., 2005) or even conscious awareness (Whalen et al., 1998). However, this more automatic amygdala response is posited to occur very quickly, and would therefore likely be observed as activity in the first time point after picture onset. It is possible that the sustained amygdala response observed later in the trial is dependent upon the continued direction of attention to the emotional features in the stimulus, as proposed above.

The present model posits a large positive path from IFG to ACC during the look negative condition. The present interpretation of that path is that it represents the task-appropriate facilitation of attention towards emotion. This leads to the hypothesis that if the instructions and trial structure were set up in a way that did not emphasize attention towards emotion in the look negative condition, this path would not be as strongly positive. For example, participants in the present study were instructed to respond naturally to the images and be aware of their emotional response. In addition, on every trial they were asked to rate their strength of negative affect directly after viewing each picture. Because the last 6 seconds of the picture-viewing period were considered for the model here, it is possible that some of the activity represents their preparation for making that rating, which would certainly involve directing attention towards subjective experience.

The present interpretation highlights two components of emotion regulation that are potentially identified by the present results. The first component involves the implementation of control via task-appropriate allocation of attention towards emotion. The second component involves the ongoing negative feedback between attention

towards emotional experience and the subjective emotional experience itself. It is unclear whether these components must necessarily work together to achieve successful emotion regulation. The first component, (implementation of regulation), would result in decreases in activity from both the amygdala and the insula if executed in isolation. The second component (change in subjective experience), could potentially occur independently of the implementation of regulation, but is here observed in concert with it.

It is possible that these two processes represent separable mechanisms of regulation. If this is true, future research may clarify whether one or both of these processes are necessary for successful emotion regulation to occur. These two processes may be more or less successful when used in different contexts or by different individuals. In addition, investigating the nature of these processes may help pave the way for more effective treatments for mood and anxiety disorders that are characterized by emotion dysregulation.

The first process involves the implementation of regulation, and is represented by the path from IFG to ACC. The ability to recruit this attentional region in accordance with task goals might be considered part of broader cognitive control abilities. Executive function or cognitive control in general is posited to be impaired in individuals with major depressive disorder (Landro, Stiles, & Sletvold, 2001; Veiel, 1997; Weiland-Fiedler et al., 2004). If changes in this path alone are responsible for regulation-related decreases in amygdala and insula activity, one might predict that training in cognitive control more generally would result in increased effectiveness of emotion regulation efforts. This notion is consistent with the observation that improvements due to cognitive

therapy are associated with changes in the interaction between cortico-cortical connections as opposed to limbic or cortico-limbic changes (Paquette et al., 2003; Seminowicz et al., 2004). In addition, there are preliminary reports that interventions targeting general executive functioning skills can facilitate cognitive control when used for the purpose of emotion regulation (Siegle, Ghinassi, & Thase, in press).

On the other hand, the reciprocal paths from insula to ACC may represent the degree to which individuals can curtail the positive feedback between subjective emotional experience and attention to that emotional experience. Modulation of these paths may be difficult for individuals who have difficulty in directing attention away from internal experience or visceral sensations, such as individuals with generalized anxiety or ruminative depression. Therefore, interventions targeted directly at changing one's subjective experience may be more effective for individuals who display dysregulation of this type.

Limitations and Future Directions

There are several limitations to the present study. Because the present goal was to maximize the power available to differentiate between negative and neutral stimuli, we were unable to test for sex differences, despite evidence that men and women respond differently to emotional stimuli, as shown by self-reported negative affect (Bradley, Codispoti, Sabatinelli, & Lang, 2001), sex differences in emotion cue processing (Feldman Barrett, Lane, Sechrest, & Schwartz, 2000; Nolen-Hoeksema & Jackson, 2001), psychophysiological measures (Bradley et al., 2001), and functional neuroimaging

studies (Butler et al., 2005; Cahill et al., 2001; Gur et al., 1995; Kilpatrick et al., 2006; Wrase et al., 2003).

The present study did not take full advantage of the time-course information available in this event-related fMRI dataset. In accordance with previous subtraction-based analyses of the cognitive regulation of emotion, the PLS and SEM analyses used data from the picture-viewing period only. Subsequently, the data from the three timepoints that were not used as a reference scan (lags 1-3) were averaged to create the covariate used in the right amygdala seed PLS. In the future, investigating the functional and effective connectivity between regions during the instruction period might shed light on the preparatory processes that occur before the presentation of an emotional stimulus. In addition, the time period immediately following the picture-viewing period (when participants were making negative affect ratings) can be investigated. Including instruction and ratings periods may allow for enough time points to look for the influence of one region early in the trial on other regions later in the trial. A similar approach has recently been used to characterize differences in the time course of different types of emotion regulation strategies (Goldin et al., in press).

For the SEMs presented in this report, models were restricted to the right hemisphere. This has important limitations when considering the laterality of the control regions and the emotion-responsive regions in the model. Many studies of the cognitive control of emotion report regulation-related activity primarily in left-sided prefrontal regions, which suggests that the present approach focusing on the right hemisphere may be unnecessarily conservative (Ochsner & Gross, 2005). In addition, models of

hemispheric asymmetry in emotion suggest a greater role for left prefrontal cortex in diminishing negative emotion (Jackson et al., 2003). However, activations in inferior portions of the right lateral prefrontal cortex have been noted in studies of effortful emotion regulation (Ochsner et al., 2004; Phan et al., 2002). In addition, this right-sided region has been hypothesized to be engaged during tasks when emotion labeling may have a down-regulatory function (Hariri et al., 2000; Taylor et al., 2006).

Several theories of amygdala laterality may also be pertinent to the selection of hemisphere in this study. There is some evidence that the right amygdala responds preferentially to visual stimuli, even when presented below conscious awareness, and habituates quickly. By contrast, the left amygdala is thought to respond to verbal stimuli, maintain activity longer than the right, and respond more robustly to supraliminally presented stimuli (Morris, Öhman, & Dolan, 1999; Phelps et al., 2001; Williams et al., 2005). The present study reports regulation-related decreases in right, but not left amygdala during the cognitive regulation of emotion. It is unclear how the cognitive regulation of visual stimuli might map onto these left-right distinctions, and may seem counter-intuitive that the right amygdala is implicated here, given the long exposure duration of each emotional stimulus. However, no condition x hemisphere analyses were conducted to test hemispheric specificity. In the future, the stacked model approach can be used to test for the appropriateness of this model in the left hemisphere. Other investigations of functional and effective connectivity of emotional processing have found that models created in one hemisphere are also appropriate for the other (de Marco

et al., 2006) although others report differential connectivity using seeds from the different hemispheres (Das et al., 2007; Kilpatrick et al., 2006; Williams et al., 2006) .

Ratings of negative affect were taken on a trial-by-trial basis in this study, but have presently only been used to confirm that the overall pattern of negative experience was achieved. In addition, post-scan ratings of regulation difficulty and regulation strategies used were recorded. In the future, these measures can be used as covariates in a behavior PLS to investigate between-condition differences in the covariance between neural activity and these measures.

As is always the case when using SEM, only the influence of regions and paths that are included in the model can be evaluated. Therefore, the paths that significantly differ between the regulation and non-regulation conditions may not reflect the direct influence of IFG onto ACC (for example) but rather influence through another structure not included in the model. Several principles guided the selection of regions for the present study, and so the models presented here should be interpreted with these principles in mind. Regions were selected based on the previous literature and region covariation with the right amygdala in a separate PET study. This might have biased the selection of regions included in this analysis. In particular, regions more active in the PET study might reflect regions for which there is a sustained response to emotional pictures over time. In addition, the regions for the present study were derived from a seed PLS using the right amygdala as a seed voxel. Although the amygdala is a common focus for studies of negative emotion, there are other areas that are equally (if not more robustly) engaged during negative emotion. For example, the insula has been identified in

several types of negative emotion induction (Lane et al., 1997; Phillips et al., 2003; Sanfey et al., 2003; Wright, He, Shapira, Goodman, & Liu, 2004) and is thought to correspond closely with subjective affect in response to negative stimuli (Critchley et al., 2004). In addition, it observed to be commonly down-regulated in studies using cognitive reappraisal (Ochsner et al., 2002; Ochsner et al., 2004). Although the insula was included in the present model, it is important to investigate the networks identified when it and other regions are used as seeds.

Although the amygdala was the apriori region of interest for the present study, the scanning parameters employed were not optimized for targeted study of the amygdala alone. The slice prescription and scanning parameters used here were chosen to maximize the quality of signal from medial temporal regions such as the amygdala and the quality of the signal from the entire brain. If the present study were to target amygdala activation alone, several changes to the experimental task and scanning parameters would have been made. First, it has been demonstrated that tasks that involve the perception of emotional faces elicit more robust amygdala activity than tasks that use the complex visual scenes used here (Britton, Taylor, Sudheimer, & Liberzon, 2006). In addition, slices prescribed in an oblique coronal fashion (e.g., (Kim, Somerville, Johnstone, Alexander, & Whalen, 2003) are less likely to encounter signal dropout from the nasal sinus than the axial slices used in the present study, although this concern is minimized by the use of spiral acquisition sequences (Preston et al., 2004). In addition, if the present study were designed to maximize inferences made about amygdala activity alone, thinner slices would be afforded by the reduction in whole-brain coverage to allow greater spatial

resolution. Lastly, larger field strengths than those used in this study are currently available for human research (up to 7 Tesla), offering a spatial resolution as small as 1 mm.

Previous studies investigating individual differences and contextual effects on amygdala activity have distinguished between dorsal and ventral amygdala activity (Kim et al., 2003; Kim et al., 2004; Somerville, Kim, Johnstone, Alexander, & Whalen, 2004). The z = -10 boundary in Talaraich space is commonly used to roughly divide the structure into the central and basolateral amygdaloid nuclei respectively. The right amygdala peak voxel in the present study is within the ventral region, according to this convention (z = -18, MNI space, z = -15, Talairach Space). Therefore, it is plausible that this activation reflects activity of the basolateral complex (BLC). The BLC receives input from several sensory and association cortices, whereas the central nucleus appears to govern autonomic, behavioral and attentional amygdalar outputs (Aggleton, 2000; LeDoux, 1996). Activity within the BLC can be modulated by the emotional context in which a neutral stimulus is perceived (Kim et al., 2004) and by individual differences in stimulus interpretation (Kim et al., 2003) and anxiety (Somerville et al., 2004). Because the regulation strategy used in the present study involves a change in the emotional meaning of the stimuli, the present results are consistent with the notion that contextual interpretation of a stimulus can affect activity in the BLC. Regulation strategies that directly target processes associated with central nucleus output (autonomic and behavioral responses, increased vigilance towards one's environment) may similarly affect the dorsal portion of the amygdala.

The previous literature on the functional neuroanatomy of emotion and emotion regulation provided guidance at several steps in the present study. First, this literature was used to guide region selection. In addition, it was used to interpret the differences in effective connectivity between regions. However, it is still unclear how differences in functional and effective connectivity relate to subtraction-based differences in activation. It has been demonstrated that meaningful differences in functional connectivity are sometimes present when no activation differences can be detected using subtractions (Nyberg et al., 2000). Therefore, whenever possible, data from lesion studies, electrophysiology studies and other functional connectivity analyses should be used in parallel with the subtraction-based literature. More research utilizing both kinds of analyses are required before the relationship between them is clarified.

Anatomical connections for the structure of the effective connectivity models were derived from a database of studies in non-human primates (Kotter, 2004). Post-mortem studies and in vivo neuroimaging techniques indicate that anatomical connectivity may be sufficient for comparison in humans and macaques (Croxson et al., 2005; Öngür, Ferry, & Price, 2003). Because relatively little is known about anatomical connectivity in the human brain, several previous studies have used a similar approach. However, it should be noted that most previous studies were of psychological processes that may be reasonably homologous in humans and non-human primates (perception, learning, memory). The present study focuses upon the voluntary self-regulation of emotion, which is a meta-cognitive function that is difficult, if not impossible to study in non-human primates. In addition, the particular type of cognitive control studied here,

reappraisal, relies heavily upon linguistic re-interpretation of complex visual images, which calls into question the appropriate use of anatomical connectivity from non-human primates.

CONCLUSION

The present study used multivariate techniques and statistical modeling to investigate the functional and effective connectivity of the cognitive down-regulation of negative emotion. Consistent with previous reports, the cognitive regulation of emotion was associated with a significant reduction in path strength from cognitive control-related prefrontal cortex regions to emotion-related regions such as the amygdala and insula. These paths were not direct but were mediated by the anterior cingulate cortex. In particular, the path between the inferior frontal gyrus and the anterior cingulate was significantly less positive during the regulation than the non-regulation of negative affect. These results support previous interpretations of the increased activity in alleged cognitive control regions and decreased activity in purported emotion-related regions during the cognitive control of emotion. In addition, they identify the relationship between lateral prefrontal control regions and anterior cingulate regions for further investigation of the effective connectivity of emotion regulation.

APPENDIX A

Rationale

There are few reports of functional and effective connectivity during the viewing of negative and neutral stimuli by healthy participants. Therefore, to aid in the identification of regions and interpretation of results for the analyses reported in the main body of the paper, PLS and SEM were also performed upon an available data set of positron emission tomography (PET) data in 44 individuals (22 women).

The purpose of this analysis was to identify regions that significantly covary with a task involving the perception of negative and neutral pictures. It was planned to use the amygdala as a seed voxel to identify other regions that covaried positively and negatively with that seed. Lastly, structural equations modeling was performed upon these regions in order to identify differences in effective connectivity between negative and neutral picture perception.

Method

Participants

Forty-four healthy participants (22 women) completed the experimental procedure. Prospective subjects were screened by phone and excluded if they reported a history of neurological abnormalities, head injury, learning disabilities, current psychoactive medication use, current drug or alcohol abuse, current major depressive episode, lifetime incidence of bipolar or psychotic disorders, native language other than English (to ensure comprehension of instructions and questionnaires), or same-sex sexual preference (to ensure pleasant response to heterosexual erotic stimuli). Female

participants completed the procedure during the follicular phase of their menstrual cycle (days 5-11). Participants provided their written informed consent, were compensated for their participation, and were studied under the guidelines of the Institutional Review Boards (IRBs) at the Banner Good Samaritan PET Center and the University of Arizona.

Task

Six blocks of picture viewing were counterbalanced for order around two blocks of visual fixation, which were always the first and fifth scans administered in an 8-block scanning session. Picture-viewing blocks consisted of 14 images from the IAPS. Each picture was shown for 6 seconds and separated from the next picture by a cross-hair presented for one second. Because each scan began when the tracer exceeded 15% over baseline and lasted for 60 seconds, not all 14 images were viewed during data collection, but images were shown continuously throughout data collection. During the visual fixation conditions a cross-hair appeared on the screen in place of a picture. The emotional picture-viewing conditions consisted of high arousal pleasant, low arousal pleasant, high arousal unpleasant, and low arousal unpleasant images (based on normative ratings). Two neutral picture conditions consisted of one depicting human faces and another that did not (scenes and everyday objects). Because the normative ratings given by men and women diverge for highly arousing images, the 14 IAPS images were different for men and women, selected to achieve the greatest level of arousal for each group. The low arousal pleasant, low arousal unpleasant, and neutral images were identical for men and women. Subjects were given the following instruction

before each scan: “Please look at the screen and allow yourself to feel whatever each picture evokes in you.”

Brain Imaging

Positron Emission Tomography Imaging

PET was performed on an Exact HR+ scanner (Siemens, Knoxville, TN), which recorded data in the 3D mode and permitted the reconstruction of images consisting of 63 horizontal slices with a center-to-center slice separation of 2.46 mm, an axial field of view of 15.5 cm, an in-plane resolution of 4.2-5.1 mm full width at half-maximum (FWHM), and an axial resolution of 4.6-6.0 mm FWHM. Attenuation correction was performed using 2 Ge-68/Ga-68 external rod sources. Intravenous bolus injections of 15 mCi ^{15}O water were given and 60 second static scans automatically initiated as the tracer arrived at the brain and exceeded a 15% over baseline threshold. Eight scans 10-15 minutes apart were obtained for each subject during six picture viewing conditions and two visual fixation conditions.

Anatomical Imaging

T_1-weighted, volumetric MRIs were acquired using a 1.5-T Signa system (General Electric, Milwaukee) to rule out gross anatomical abnormalities and for the subsequent identification of amygdala ROIs. Sequence parameters were: 192 x 256 matrix, TR=33 ms, TE=5 ms, $a=30^0$, FOV =24 cm which resulted in 1.5 mm thick contiguous images.

Self-reported affect

Immediately following each scan, the images were replayed and subjects reported aloud their valence and arousal rating in response to each image on a 9-point scale (Bradley & Lang, 1994) based on how they experienced the picture during the first viewing.

Skin Conductance Acquisition

Skin conductance was collected using a Biopac amplifier with two Ag/AgCl electrodes attached to the participant's left palm. Data were collected at 500 Hz.

Data Analysis

Manipulation Check

Self-reported negative affect

Ratings of valence and arousal for each picture were averaged to provide a mean rating for negative and neutral scans. A within-subjects t-test in SPSS was performed to test the hypothesis that ratings of valence were more negative to the negative pictures than the neutral pictures, and another to test the hypothesis that negative images were found more arousing than neutral images.

Skin Conductance Response

SCR amplitudes were computed by identifying SCRs that begin during the 1-4 seconds of each picture presentation within the block and subtracting the proximal baseline from the maximum amplitude of the response. SCR amplitudes to each picture were averaged to create mean amplitudes for the negative and neutral picture-viewing

conditions. SCR amplitudes should provide evidence parallel to that of self-reported affect that the picture manipulation results in the greatest mean SCR amplitude during the negative condition, and significantly smaller mean SCR amplitude during the neutral condition.

Basic Contrasts

Please see man manuscript for details of pre-processing, with the exception that images were smoothed with a 12 mm FWHM kernel. Preprocessed images were entered into general linear model in SPM to create subtraction contrasts between conditions of interest (negative > neutral) for each subject. These individual contrasts were then entered into a one-sample t-test to perform a random-effects group analysis.

PLS and SEM analyses

See main manuscript for details.

Results

Manipulation check

Self-reported affect

A within-subjects t-test was performed to confirm that ratings of valence were more negative to the negative images (m=6.91) than the neutral images (m=4.90) ($t(43)= 14.45$, $p<0.001$) , and another to confirm that negative images (m=5.82) were found more arousing than neutral images (m=8.42) ($t(43) = -13.13$, $p<0.001$). These means are displayed in Figure 1.

Figure A.1. Mean ratings of valence (a) and arousal (b). ‘9’ represents most negative on the valence scale, ‘1’ represents most positive, with ‘5’ representing neutral. ‘1’ represents most highly aroused on the arousal scale, ‘9’ represents least aroused. Error bars represent standard error of the mean (SEM).

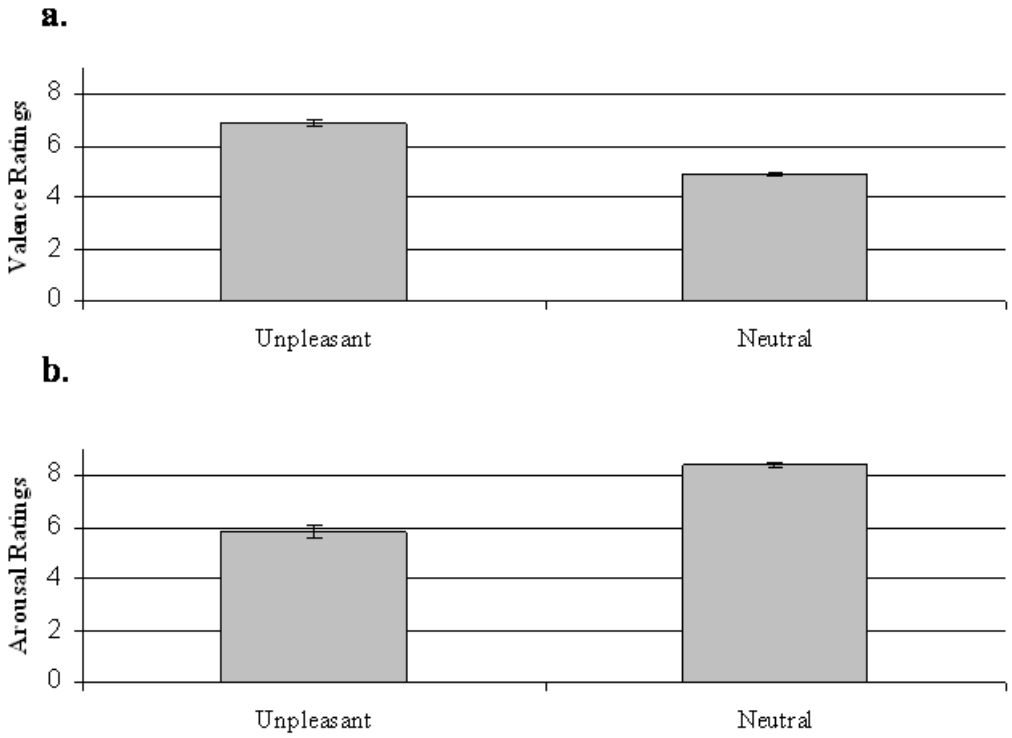

Skin Conductance Response

A within-subjects t-test was performed to confirm that the average amplitude of SCRs were greater to the negative images (m=0.55 than the neutral images (m=0.18) ($t(41)= 3.77$, $p<0.002$). SCR means are displayed in Figure 2.

Figure A.2. Mean SCR amplitude (in μSeimens). Error bars represent SEM.

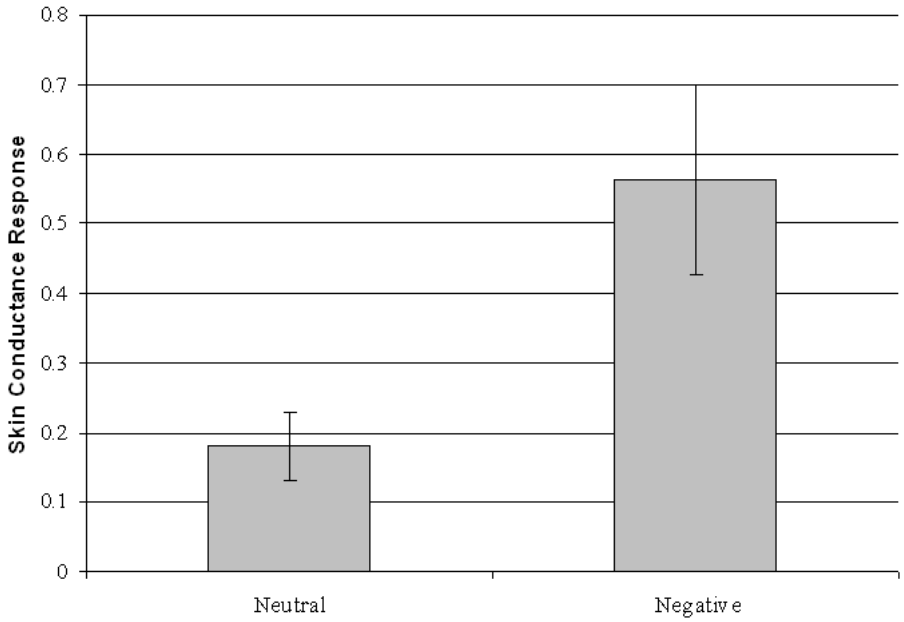

Basic Contrasts

The second-level comparison of negative (high arousal and low arousal) to neutral (faces and objects) revealed strong activations that spanned bilateral occipital cortex as well as both amygdalae and much of the surrounding parahippocampal and temporal cortices. These activations were so strong that at a threshold of $p<0.001$, uncorrected, only one peak voxel was identified, and the other clusters were included in the continuous surrounding cluster (see Figure 3).

Figure A.3. Surface rendering (a) and coronal slice (b) of negative > neutral second-level contrast in SPM (Study 1). Threshold was set to p<0.001, uncorrected.

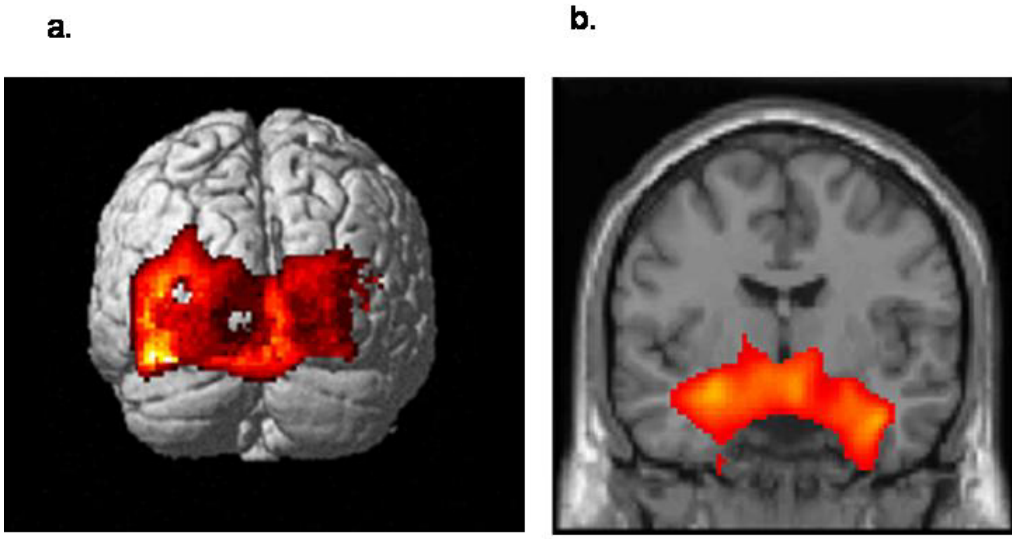

PLS

Negative and neutral scans (2 each) were entered in to a task PLS. Two participants (both females) were eliminated from the analysis due to extreme brain scores. The first two latent variables reliably explained a significant portion of the variance in the brain-task block. The first LV primarily identified regions that distinguish between the high arousal unpleasant condition and the low arousal neutral condition (objects) and accounted for 59.65% of the covariance in the brain-task block (p<0.001, see Figures 4 and 5 and Table 1).

Figure A.4. Experimental task condition weightings on LV1 for Task PLS. Conditions are depicted in the following order: high arousal negative, low arousal negative, low arousal neutral, high arousal neutral.

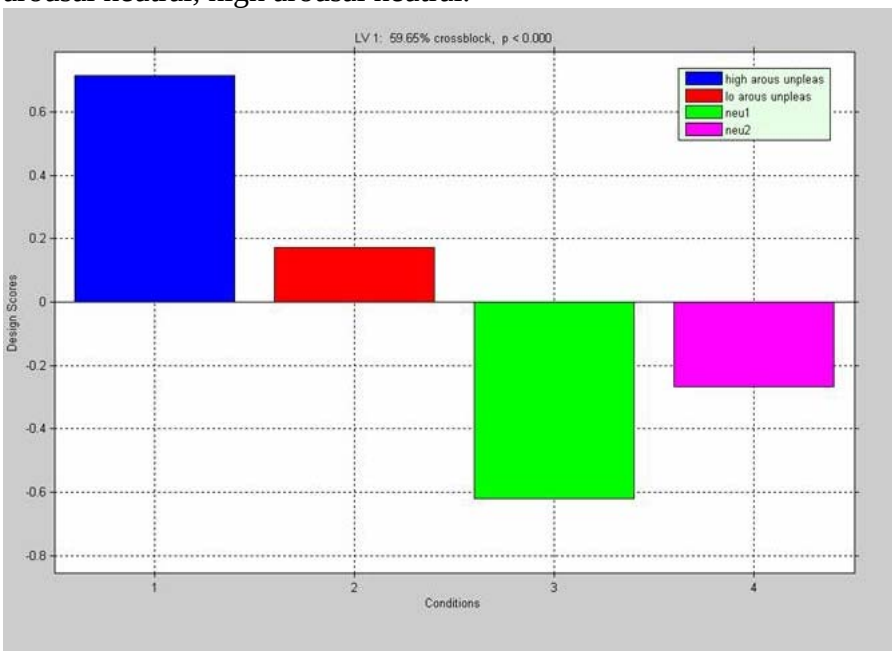

Figure A.5. LV1 for Task PLS, displayed over normalized T1-weighted anatomical image.

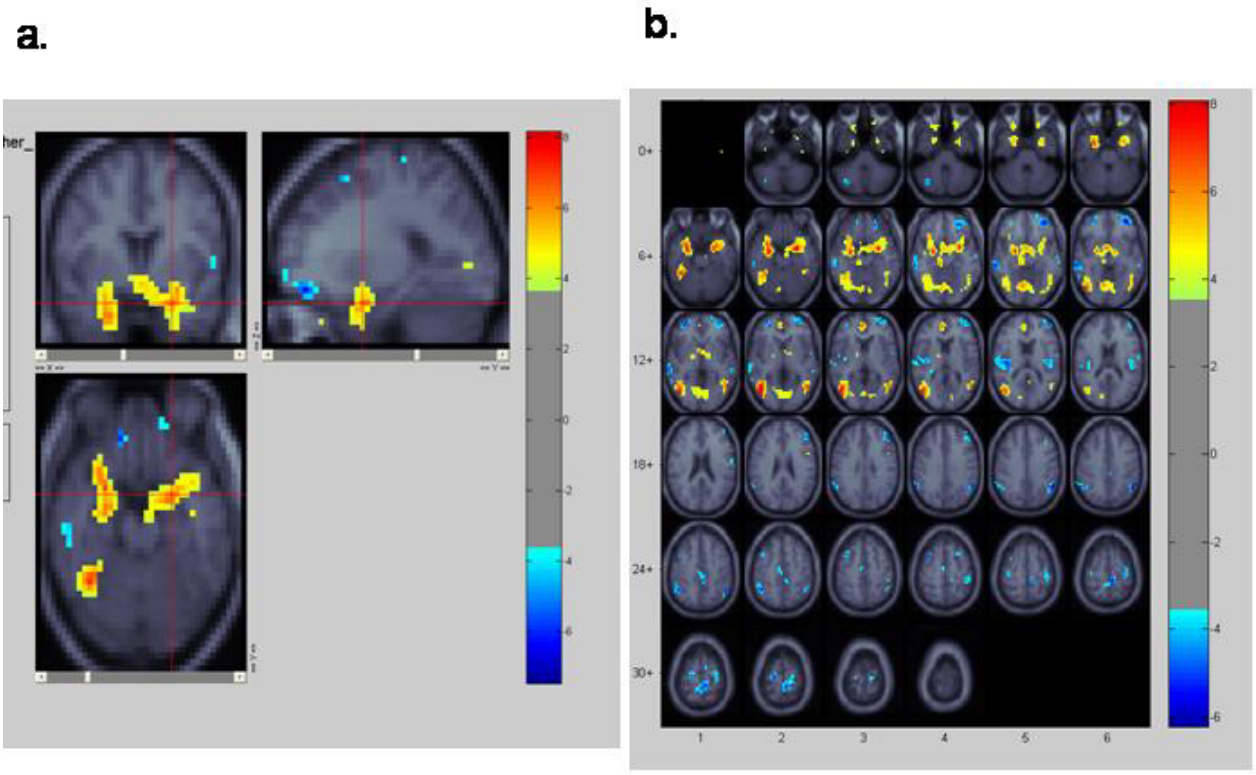

Table A.1. Clusters for LV1, Task PLS (PET study)

X	Y	Z	BSR	Cluster Size	B.A.	Region	Lobe
-44	-72	0	8.09	486	B.A. 37	Middle Occipital Gyrus	Occipital Lobe
-28	-8	-20	7.91	602	N/A	Lateral Ventricle	Sub-lobar
48	-64	-4	6.46	113	N/A	Middle Temporal Gyrus	Temporal Lobe
-4	48	4	6.11	37	B.A. 32	Anterior Cingulate	Limbic Lobe
20	36	-36	4.84	21	N/A	N/A	N/A
-28	32	-36	4.69	24	N/A	N/A	N/A
-16	-84	16	4.17	6	B.A. 18	Cuneus	Occipital Lobe
52	-52	36	-6.23	42	B.A. 40	Supramarginal Gyrus	Parietal Lobe
36	44	-12	-5.64	155	B.A. 11	Middle Frontal Gyrus	Frontal Lobe
8	-36	64	-5.51	72	B.A. 6	Paracentral Lobule	Frontal Lobe
-32	52	-4	-5.46	26	B.A. 10	Middle Frontal Gyrus	Frontal Lobe
-44	-52	48	-5.39	54	B.A. 40	Inferior Parietal Lobule	Parietal Lobe
-40	-24	12	-5.32	62	B.A. 41	Transverse Temporal Gyrus	Temporal Lobe
-20	-24	72	-5.30	14	B.A. 6	Precentral Gyrus	Frontal Lobe
-64	-36	-12	-5.28	66	B.A. 21	Middle Temporal Gyrus	Temporal Lobe
-36	8	56	-5.09	15	B.A. 6	Middle Frontal Gyrus	Frontal Lobe
-36	-72	-44	-5.03	14	N/A	Pyramis	Cerebellum
32	-16	64	-4.79	41	B.A. 6	Precentral Gyrus	Frontal Lobe
4	-36	44	-4.76	28	B.A. 31	Cingulate Gyrus	Limbic Lobe
44	-20	12	-4.55	24	B.A. 13	Insula	Sub-lobar
-64	-52	-4	-4.51	6	N/A	Middle Temporal Gyrus	Temporal Lobe
-36	-24	60	-4.30	6	B.A. 4	Precentral Gyrus	Frontal Lobe

This analysis revealed several regions that have been previously implicated in negative emotional responsivity (Table 1 and Figure 5). The second LV primarily identified regions that distinguish between the low arousal unpleasant condition and the high arousal neutral condition (faces) and accounted for 26.85% of the covariance ($p<0.020$, see Table 2 and Figure 6).

Figure A.6. Experimental task condition weightings on LV2 for Task PLS. Conditions are depicted in the following order: high arousal negative, low arousal negative, low arousal neutral, high arousal neutral.

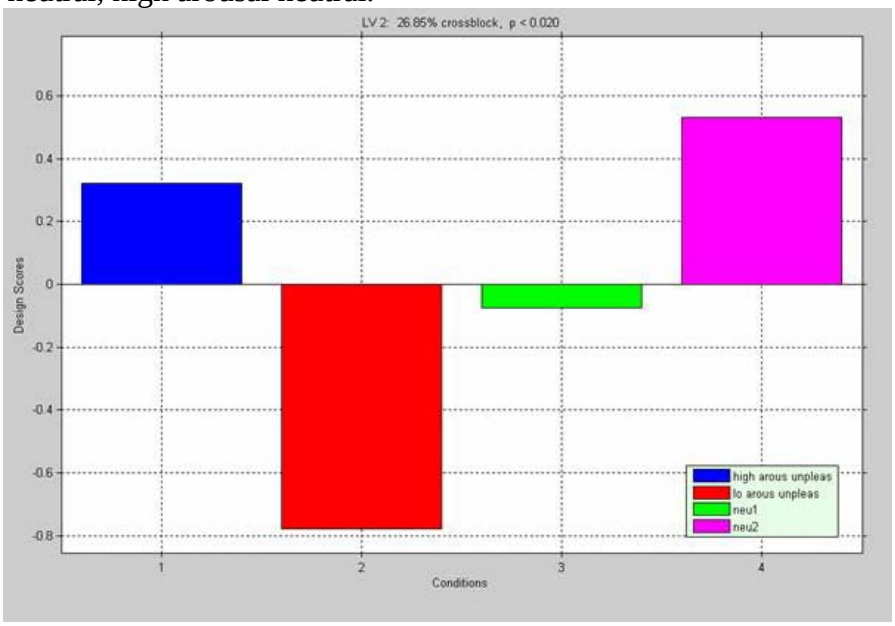

Table A.2. Clusters for LV2, Task PLS. (PET study)

X	Y	Z	BSR	Appro.P	Cluster Size	B.A.	Region	Lobe
-52	-28	40	4.94	0	138	B.A.2	Postcentral Gyrus	Parietal
-16	60	-16	4.87	0	142	B.A.11	Superior Frontal Gyrus	Frontal
-20	36	36	4.76	0	188	B.A.9	Superior Frontal Gyrus	Frontal
-28	8	44	4.54	0	99	B.A.8	Middle Frontal Gyrus	Frontal
52	12	-4	4.44	0	131	B.A.22	Superior Temporal Gyrus	Temporal
0	-12	-32	4.03	0.0001	68	N/A	N/A	Pons
32	4	-8	3.93	0.0001	23	N/A	Claustrum	Sub-lobar
24	-36	56	3.86	0.0001	124	B.A.3	Postcentral Gyrus	Parietal
12	28	24	3.52	0.0004	117	B.A.32	Anterior Cingulate	Limbic
-28	-64	-40	3.44	0.0006	33	N/A	Pyramis	Cerebellum
64	-24	-28	3.43	0.0006	11	N/A	N/A	N/A
48	44	0	3.32	0.0009	21	N/A	Inferior Frontal Gyrus	Frontal
12	-32	40	3.25	0.0011	45	B.A.31	Cingulate Gyrus	Limbic
-52	-24	-8	3.01	0.0026	25	B.A.21	Middle Temporal Gyrus	Temporal
-24	-52	44	2.97	0.003	16	B.A.7	Precuneus	Parietal
-48	0	-4	2.94	0.0033	17	B.A.22	Superior Temporal Gyrus	Temporal
32	0	36	2.92	0.0035	33	B.A.6	Precentral Gyrus	Frontal
4	-24	-12	2.90	0.0037	11	N/A	N/A	Midbrain
32	52	-12	2.69	0.0072	18	B.A.11	Middle Frontal Gyrus	Frontal
-12	-28	56	2.66	0.0079	8	B.A.6	Medial Frontal Gyrus	Frontal
40	-80	8	-7.59	0	849	B.A.19	Middle Occipital Gyrus	Occipital
-32	-88	8	-7.06	0	822	B.A.18	Middle Occipital Gyrus	Occipital
-20	36	-40	-3.87	0.0001	14	N/A	N/A	N/A
20	-16	-24	-3.83	0.0001	13	N/A	Parahippocampall Gyrus	Limbic
-8	-20	80	-3.35	0.0008	21	B.A.6	Precentral Gyrus	Frontal
8	-48	72	-3.27	0.0011	39	B.A.7	Postcentral Gyrus	Parietal
-4	12	72	-3.27	0.0011	21	N/A	N/A	N/A
-36	-16	-32	-3.15	0.0016	6	B.A.20	Uncus	Limbic
-12	-12	-16	-3.04	0.0024	8	N/A	N/A	Midbrain
-36	-48	72	-2.89	0.0039	6	N/A	N/A	N/A
20	12	-4	-2.83	0.0046	7	Putamen	Lentiform Nucleus	Sub-lobar
-12	-56	64	-2.71	0.0068	14	B.A.7	Precuneus	Parietal
20	-76	36	-2.67	0.0075	12	B.A.7	Precuneus	Parietal

Because we had an apriori interest in the connectivity of the amygdala, we chose the peak voxel in right amygdala for a seed analysis. The right amygdala seed PLS identified several of the same regions that distinguished between negative and neutral conditions in the task PLS. Left amygdala, ACC, and several visual areas covaried positively with the right amygdala seed. Several prefrontal areas as well as lingual gyrus and precuneus, covaried negatively with the right amygdala seed (see Figure 7).

Figure A.7. LV1 for right amygdala seed PLS, displayed over normalized T1-weighted anatomical image.

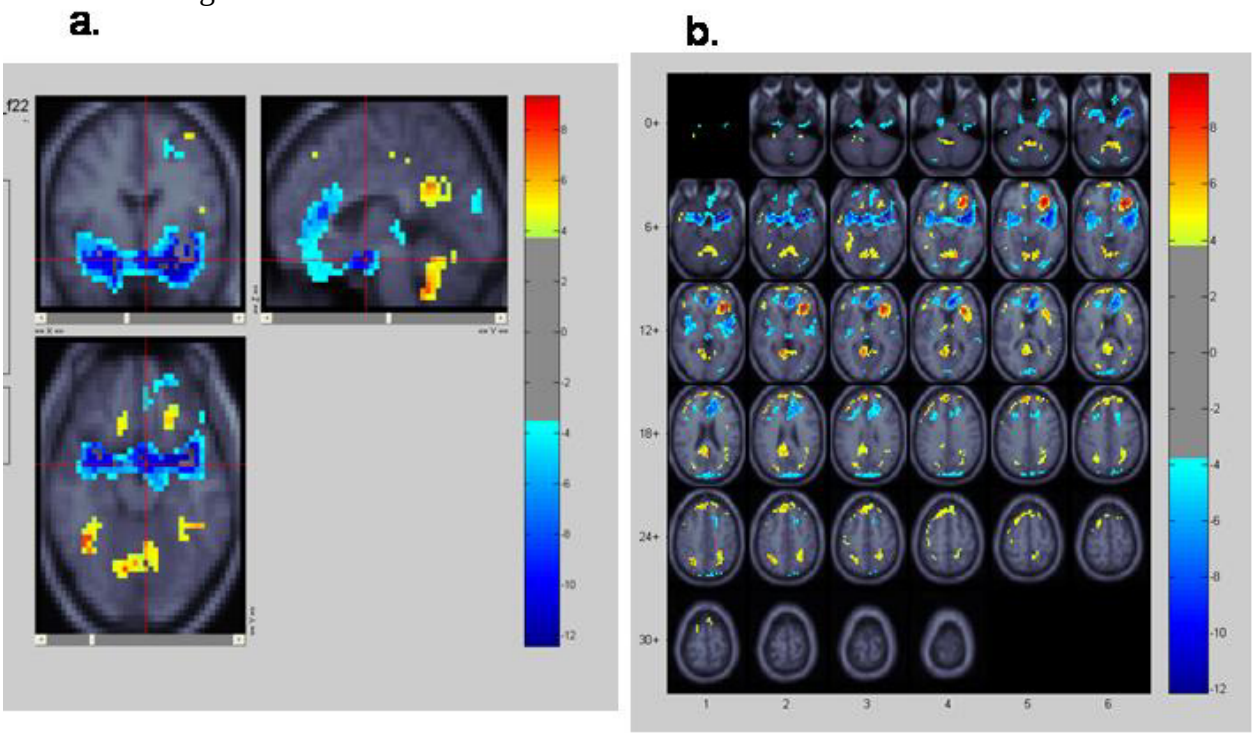

Table A.3. Clusters for LV1, right amygdala seed PLS (PET study). Regions in bold face were selected for inclusion in the SEMs.

X	Y	Z	BSR	Cluster Size	B.A.	Region	Lobe
28	**28**	**-8**	**9.96**	**239**	**B.A. 47**	**Inferior Frontal Gyrus**	**Frontal**
-28	-64	44	7.94	43	B.A. 7	Superior Parietal Lobule	Parietal
-12	-56	0	7.89	355	B.A. 18	Lingual Gyrus	Occipital
-12	56	28	7.03	281	B.A. 9	Superior Frontal Gyrus	Frontal
24	**-72**	**36**	**6.70**	**90**	**B.A. 7**	**Precuneus**	**Parietal**
-44	-56	-16	6.45	30	B.A. 37	Fusiform Gyrus	Temporal
-44	32	24	6.25	27	B.A. 46	Middle Frontal Gyrus	Frontal
-28	-76	24	6.04	22	N/A	Sub-Gyral	Occipital
36	-48	20	5.47	10	N/A	Extra-Nuclear	Sub-lobar
-12	**20**	**-16**	**5.31**	**13**	**B.A. 25**	**Medial Frontal Gyrus**	**Frontal**
24	-76	24	4.96	9	B.A. 18	Precuneus	Parietal
-16	-12	12	4.85	14	Ventral Lateral Nucleus	Thalamus	Sub-lobar
20	64	8	4.45	10	B.A. 10	Medial Frontal Gyrus	Frontal
32	**4**	**-24**	**-12.13**	**918**	**B.A. 28**	**Uncus**	**Limbic**
4	**36**	**4**	**-9.44**	**503**	**N/A**	**Anterior Cingulate**	**Limbic**
24	-96	20	-7.91	126	B.A. 19	Cuneus	Occipital
0	-28	-4	-6.92	23	N/A	N/A	Midbrain
36	-20	-44	-6.76	31	N/A	N/A	N/A
-24	40	4	-6.67	113	N/A	Sub-Gyral	Frontal
28	-84	-12	-6.35	48	B.A. 18	Middle Occipital Gyrus	Occipital
-28	-84	-36	-6.07	8	N/A	Uvula	Cerebellum Posterior
-28	-88	-12	-5.64	9	B.A. 18	Inferior Occipital Gyrus	Occipital
-28	44	-20	-5.39	15	N/A	N/A	N/A

Selection of regions

Regions that showed significant functional covariance with the right amygdala seed were selected for inclusion in the SEM based on the previous literature. The regions chosen that covaried positively with the amygdala seed were the insula, subgenual anterior cingulate (sACC), and the anterior cingulate cortex (ACC, a large activation that

spanned rostral and dorsal regions). The regions chosen that covaried negatively with the right amygdala seed were the inferior frontal gyrus (IFG), superior frontal gyrus (SFG) and the precuneus. The insula has a documented role in the processing of several types of negative emotion, and is often thought to be primarily engaged during the experience of disgust (Critchley et al., 2004; Lane et al., 1997; Phan et al., 2002; Phillips et al., 2003; Sanfey et al., 2003; Vaitl et al., 2005). The subgeneual cingulate cortex has been shown to be engaged in particular during the experience of sadness, and is thought to be a crucial node in a network that is abnormal in major depressive disorder (Kumari et al., 2003; Mayberg et al., 1999; Mayberg et al., 2005). The anterior cingulate cortex is thought to be engaged by both cognitive and emotional tasks, is active while directing attention towards emotionally-relevant stimuli experience (Carretié, Hinojosa, Martín-Loeches, Mercado, & Tapia, 2004; Hutcherson et al., 2005), and is also a key region in current conceptualizations of cognitive control. The precuneus is commonly more active during the processing of emotional than neutral visual or imagined stimuli, although often more active during the processing of positive stimuli (Gilboa, Winocur, Grady, Hevenor, & Moscovitch, 2004; Goldin et al., 2005; Habel, Klein, Kellermann, Shah, & Schneider, 2005; Paradiso et al., 1999; Teasdale et al., 1999). The inferior frontal gyrus has been implicated in studies cognitive control (Amunts & von Cramon, 2006), particularly during tasks requiring motor inhibition (Garavan et al., 2006; Ray Li et al., 2006; Rubia et al., 2003).

SEMs

Peak voxel values were extracted from the selected regions and mean-corrected using the mean across all eight experimental conditions. Mean-corrected values from the two negative and two neutral conditions were averaged to create separate correlation matrices for the negative and neutral conditions.

The paths included in the SEM were based on non-human primate connectivity data available in an online database (Kotter, 2004). The stacked model in LISREL indicated better model fit when paths were free to differ between the negative and neutral conditions ($\chi^2_{diff}(28) = 55.54$, $p<0.002$). Testing each path stepwise indicated that 5 paths significantly affected differential model fit. Differential χ^2 are listed in Table 4. Final differential model fit was significant ($\chi^2_{diff}(5) = 28.67$, $p<0.0001$). Depicted in Figure 8 are the models for the negative and neutral conditions when paths identified in Table 4 were allowed to vary between conditions.

Table A.4. Significantly different paths from SEM. (PET study).
Negative vs. Neural

from	to	χ^2	negative	neutral
amyg	sACC	4.43	-0.31	0.04
SFG	rACC	5.2	0.09	-0.27
IFG	rACC	11.63	-0.08	0.29
rACC	IFG	10.75	-0.08	0.07
rACC	sACC	9.25	-0.02	0.26

Figure A.8. SEM. Lines in red indicate paths that differ significantly between the negative and neutral conditions.

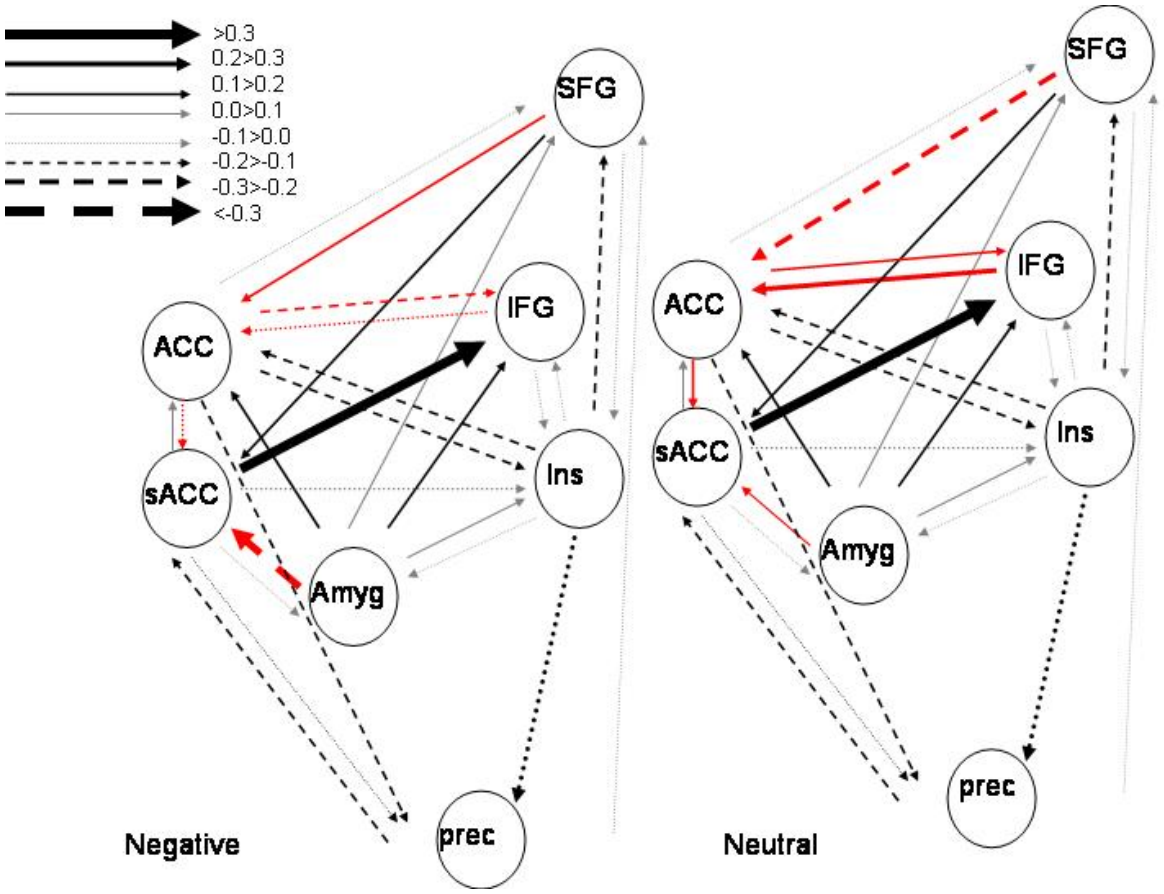

The SEMs performed upon a subset of these regions indicated that the effective connectivity between these regions was significantly different for negative and neutral conditions. In particular, the path between SFG and ACC was less negative (and slightly positive) during the negative condition than the neutral condition. In addition, the reciprocal paths between IFG and ACC were more negative during negative than neutral conditions. In addition, the path between the ACC and the sACC was more inhibitory during the negative than the neutral condition. Lastly, the path from the amygdala to sACC was more inhibitory during the negative than the neutral condition.

Considerations

Multivariate analyses with a seed voxel in the right amygdala identified seven regions that were then included in the subsequent SEMs. The key regions for which effective connectivity differed between the negative and neutral conditions were the SFG, the IFG, ACC, amygdala, and sACC. In this model the efferent connections from the ACC to emotion-responsive regions (insula and sACC) are inhibitory, particularly during the negative condition. Therefore, the difference between the conditions is characterized by greater values in afferent paths to the ACC that result in more negative efferent paths to emotion-responsive regions. Considering that several of these regions are more responsive overall to negative than neutral conditions, this result is somewhat counter-intuitive. Potential explanations for this are offered later in the discussion.

In the present data set, because our goal was to maximize arousal for all participants, men and women viewed different high arousal negative pictures in the PET study, which might constitute different discrete emotional categories (Bradley et al., 2001). Furthermore, the role that arousal plays in effective connectivity is unknown. Because the seed region was chosen from an LV that weighted strongly on the high arousal negative condition, but seed data were averaged for both negative conditions, the resulting models of effective connectivity might average across meaningful differences between the arousal conditions. Future work is planned that will potentially clarify the role of both valence and arousal in this dataset, using all eight experimental conditions.

Relation of PET data to fMRI data

In addition to the influence of arousal mentioned above, the differences in effective connectivity between data presented in this appendix and data presented in the main report might be due to differences in block versus event-related stimulus presentation (Schafer, Schienle, & Vaitl, 2005). In the PET study, the regions identified by the PLS may not be more active because of the repeated response to each stimulus in the block, but rather due to a negative mood effect that persisted over the entire one-minute scan. By contrast, the regions identified in the fMRI study most likely represent the average response to each event-related trial in each condition. Physiologically, the regions identified in the PET study may reflect regions that are able to maintain sustained activity over the course of the block, whereas regions identified in the fMRI study reflect regions that consistently respond in an event-related fashion over the course of the experiment.

In addition, the instructions for the two studies differed in a way that might affect results reported here. In the PET study, individuals were instructed to allow themselves to feel whatever each picture evoked in him or her. In the fMRI study, individuals were instructed to view each picture and respond naturally. Although these instructions may seem similar, they were given in different experimental contexts. In the PET study, individuals were seeing blocks of negative, positive, or neutral pictures and blocks of visual fixation. Therefore, the negative pictures were only one of two expected valences. In the fMRI study, the “respond naturally” instruction was a counterpoint to the instruction to use cognitive reappraisal, and only neutral and negative pictures were

presented. Directly after the scanning session, participants were asked to report on the strategies they used to implement the decrease instruction, but they were not asked to report what they did during the non-regulation (look) instruction. However, during the task training, a few subjects volunteered that during the "look" instruction, they actively reminded themselves to not reappraise. Therefore, an individual who naturally would naturally reappraise some of the negative images might still engage in that reappraisal under the instructions for the PET study, but might refrain from reappraisal during the "look" condition in the fMRI study. To investigate this possibility in the future, individual differences in emotion regulation habits, or post-scan debriefing on how participants followed the instructions might allow for the creation of high and low uninstructed regulation samples. This would allow test the hypothesis that differences between regulation and non-regulation instructions may be observed in certain individuals or populations, even without an explicit regulation instruction.

APPENDIX B

Table B.1 Negative pictures from the IAPS presented the PET study. Valence and arousal means are from normative ratings. Lines in boldface indicate that picture was also used in the fMRI study.

Description	Slide number	Valence mean	Arousal mean
High Arousal			
Snake	1120	3.79	6.93
Mutilation	3010	1.71	7.16
BurnVictim	3053	1.31	6.91
Mutilation	3069	1.7	7.03
DeadBody	3120	1.56	6.84
BabyTumor	3170	1.46	7.21
Injury	3266	1.56	6.79
SeveredHand	3400	2.35	6.91
AimedGun	6230	2.37	7.35
SlicedHand	9405	1.83	6.08
Soldier	9410	1.51	7.07
Dog	**9570**	**1.68**	**6.14**
Cat	**9571**	**1.96**	**5.64**
NativeBoy	2730	2.45	6.8
Mutilation	3000	1.45	7.26
Mutilation	3071	1.88	6.86
Mutilation	3080	1.48	7.22
BurnVictim	3110	1.79	6.7
Knife	**6300**	**2.59**	**6.61**
Attack	6350	1.9	7.29
Fire	8485	2.73	6.46
Low Arousal			
Roaches	1275	3.3	4.81
Hospital	**2205**	**1.95**	**4.53**
Girl	2381	5.25	3.04
Bum	2750	2.56	4.31
DistressedFem	6311	2.58	4.95
Cemetery	9000	2.55	4.06
Heroin	9102	3.34	4.84
Puddle	9110	3.76	3.98
Horses	9182	3.52	4.98
Woman	9190	3.9	3.91
Garbage	9290	2.88	4.4
Pollution	9342	2.85	4.49
DentalExam	9584	3.34	4.96
	HiArous Mean	1.955238095	6.821904762
	LoArous Mean	3.213846154	4.404615385

Table B.2 Neutral pictures from the IAPS presented the PET study. Valence and arousal means are from normative ratings. Lines in boldface indicate that picture was also used in the fMRI study.

Description	Slide number	Valence mean	Arousal mean
High Arousal			
Outlet	**6150**	**5.08**	**3.22**
Towel	**7002**	**4.97**	**3.16**
Mug	**7009**	**4.93**	**3.01**
Stool	**7025**	**4.63**	**2.71**
Baskets	7041	4.99	2.6
Book	**7090**	**5.19**	**2.61**
FireHydrant	**7100**	**5.24**	**2.89**
Umbrella	7150	4.72	2.61
ClothesRack	7217	4.82	2.43
Plate	**7233**	**5.09**	**2.77**
Chair	**7235**	**4.96**	**2.83**
Cabinet	7705	4.77	2.65
Tissue	**7950**	**4.94**	**2.28**
Low Arousal			
Man	**2190**	**4.83**	**2.41**
NeutFace	**2200**	**4.79**	**3.18**
Secretary	2383	4.72	3.41
Girl	**2385**	**5.2**	**3.64**
Factoryworker	2393	4.87	2.93
NeutralGirl	**2441**	**4.64**	**3.62**
ElderlyMan	**2480**	**4.77**	**2.66**
NeutralMale	2499	5.34	3.08
ElderlyWoman	**2516**	**4.9**	**3.5**
Man	2570	4.78	2.76
Women	2595	4.88	3.71
Chess	**2840**	**4.91**	**2.43**
Boy	9070	5.01	3.63
	HiArous Mean	4.948461538	2.751538462
	LoArous Mean	4.895384615	3.150769231

Table B.3 Negative pictures from the IAPS presented in the fMRI study. Valence and arousal means are from normative ratings. Lines in boldface indicate that picture was also used in the PET study.

Description	Slide number	Valence mean	Arousal mean
Baby	2053	2.47	5.25
Hospital	**2205**	**1.95**	**4.53**
SadChild	2800	1.78	5.49
Mutilation	3030	1.91	6.76
Mutilation	3051	2.3	5.62
EyeDisease	3160	2.63	5.35
BatteredFem	3180	1.92	5.77
DyingMan	3230	2.02	5.41
OpenChest	3250	3.78	6.29
Attack	3500	2.21	6.99
Attack	3530	1.8	6.82
Aimedgun	6190	3.57	5.64
AimedGun	6210	2.95	6.34
Attack	6211	3.62	5.9
AimedGun	6250	2.83	6.54
AimedGun	6260	2.44	6.93
Knife	**6300**	**2.59**	**6.61**
Abduction	6312	2.48	6.37
Attack	6370	2.7	6.44
Attack	6510	2.46	6.96
Guns	6830	2.82	6.21
Police	6831	2.59	5.55
Boxer	8230	2.95	5.91
Needles	9007	2.49	5.03
StarvingChild	9040	1.67	5.82
PlaneCrash	9050	2.43	6.36
OilFires	9120	3.2	5.77
Cow	9140	2.19	5.38
Seal	9180	2.99	5.02
DeadCows	9181	2.26	5.39
WarVictim	9250	2.57	6.6
Dirty	9300	2.26	6
Vomit	9320	2.65	4.93
Soldier	9400	2.5	5.99
Soldier	9420	2.31	5.69
Soldier	9421	2.21	5.04
Burial	9430	2.63	5.26
Skulls	9440	3.67	4.55
Ruins	9470	3.05	5.05
Corpse	9490	3.6	5.57
Boys	9530	2.93	5.2
Dog	**9570**	**1.68**	**6.14**

Cat	**9571**	**1.96**	**5.64**
Ship	9600	2.48	6.46
PlaneCrash	9611	2.71	5.75
Shipwreck	9620	2.7	6.11
Jet	9622	3.1	6.26
CarAccident	9910	2.06	6.2
CarAccident	9911	2.3	5.76
Fire	9921	2.04	6.52
	Mean	2.5482	5.8634

Table B.4 Neutral pictures from the IAPS presented in the fMRI study. Valence and arousal means are from normative ratings. Lines in boldface indicate that picture was also used in the PET study.

Description	Slide number	Valence mean	Arousal mean
Man	**2190**	**4.83**	**2.41**
NeutFace	**2200**	**4.79**	**3.18**
NeutFace	2210	4.38	3.56
SadFace	2230	4.53	4.13
Kids	2278	3.36	4.55
Boy	2280	4.22	3.77
Mother	2312	3.71	4.02
Girl	**2385**	**5.2**	**3.64**
NeutGirl	2440	4.49	2.63
NeutralGirl	**2441**	**4.64**	**3.62**
ElderlyMan	**2480**	**4.77**	**2.66**
NeutralMale	2493	4.82	3.34
ElderlyWoman	**2516**	**4.9**	**3.5**
Chess	**2840**	**4.91**	**2.43**
Outlet	**6150**	**5.08**	**3.22**
Towel	**7002**	**4.97**	**3.16**
Spoon	7004	5.04	2
Bowl	7006	4.88	2.33
Mug	**7009**	**4.93**	**3.01**
Stool	**7025**	**4.63**	**2.71**
DustPan	7040	4.69	2.69
HairDryer	7050	4.93	2.75
Book	**7090**	**5.19**	**2.61**
FireHydrant	**7100**	**5.24**	**2.89**
Lamp	7175	4.87	1.72
Clock	7211	4.81	4.2
Plate	**7233**	**5.09**	**2.77**
Chair	**7235**	**4.96**	**2.83**
Tissue	**7950**	**4.94**	**2.28**
Rain	9210	4.53	3.08
	Mean	4.744333333	3.056333333

REFERENCES

Aggleton, J. (Ed.). (2000). *The amygdala: A functional analysis*. New York: Guilford Press.

Amunts, K., & von Cramon, D. Y. (2006). The anatomical segregation of the frontal cortex: What does it mean for function? *Cortex, 42*, 525-528.

Anderson, A. K., Christoff, K., Panitz, D., De Rosa, E., & Gabrieli, J. D. E. (2003). Neural correlates of the automatic processing of threat facial signals. *Journal of Neuroscience, 23*, 5627-5633.

Anderson, A. K., & Phelps, E. A. (2001). Lesions of the human amygdala impair enhanced perception of emotionally salient events. *Nature, 411*, 305-309.

Aron, A. R., Fletcher, P. C., Bullmore, E. T., Sahakian, B. J., & Robbins, T. W. (2003). Stop-signal inhibition disrupted by damage to right inferior frontal gyrus in humans. *Nature Neuroscience, 6*, 115-116.

Beck, A. T., Rush, S., Shaw, P., & Emery, N. (1979). *Cognitive therapy of depression*. New York: Guilford Press.

Bedrosian, R. C., & Beck, A. T. (1980). *Principles of cognitive therapy*. New York: Plenum Press.

Botvinick, M. M., Cohen, J. D., & Carter, C. S. (2004). Conflict monitoring and anterior cingulate cortex: An update. *Trends in Cognitive Sciences, 8*, 539-546.

Bradley, M. M., Codispoti, M., & Lang, P. J. (2006). A multi-process account of startle modulation during affective perception. *Psychophysiology, 43*, 486-497.

Bradley, M. M., Codispoti, M., Sabatinelli, D., & Lang, P. J. (2001). Emotion and motivation II: Sex differences in picture processing. *Emotion, 1*, 300-319.

Bradley, M. M., & Lang, P. J. (1994). Measuring emotion: The self-assessment manikin and the semantic differential. *Journal of Behavior Therapy: Experimental Psychiatry, 25*, 49-59.

Brass, M., & Cramon, D. Y. v. (2004). Decomposing components of task preparation with functional magnetic resonance imaging. *Journal of Cognitive Neuroscience, 16*, 609-620.

Britton, J. C., Taylor, S. F., Sudheimer, K. D., & Liberzon, I. (2006). Facial expressions and complex IAPS pictures: Common and differential networks. *NeuroImage, 31*, 906-919.

Bush, G., Luu, P., & Posner, M. I. (2000). Cognitive and emotional influences in anterior cingulate cortex. *Trends in Cognitive Sciences, 4*, 215-222.

Butler, T., Pan, H., Epstein, J., Protopopescu, X., Tuescher, O., Goldstein, M., Cloitre, M., Yang, Y., Phelps, E., Gorman, J., LeDoux, J., Stern, E., & Silbersweig, D. (2005). Fear-related activity in subgenual anterior cingulate differs between men and women. *Neuroreport, 16*, 1233-1236.

Cacioppo, J. T., & Sandman, C. A. (1978). Physiological differentiation of sensory and cognitive tasks as a function of warning, processing demands, and reported unpleasantness. *Biological Psychology, 6*, 181-192.

Cahill, L., Haier, R. J., White, N. S., Fallon, J., Kilpatrick, L., Lawrence, C., Potkin, S. G., & Alkire, M. T. (2001). Sex-related difference in amygdala activity during

emotionally influenced memory storage. *Neurobiology of Learning and Memory, 75*, 1.

Cahill, L., Uncapher, M., Kilpatrick, L., Alkire, M. T., & Turner, J. (2004). Sex-related hemispheric lateralization of amygdala function in emotionally influenced memory: An fMRI investigation. *Learning and Memory, 11*, 261-266.

Campbell-Sills, L., & Barlow, D. H. (2007). Incorporating emotion regulation into conceptualizations and treatments of anxiety and mood disorders. In J. J. Gross (Ed.), *Handbook of emotion regulation* (pp. 542-559). New York: Guilford.

Canli, T., Qiu, M., Omura, K., Congdon, E., Haas, B. W., Amin, Z., Herrmann, M. J., Constable, R. T., & Lesch, K. P. (2006). Neural correlates of epigenesis. *Proceedings of the National Academy of Sciences of the United States of America, 103*, 16033-16038.

Carretié, L., Hinojosa, J. A., Martín-Loeches, M., Mercado, F., & Tapia, M. (2004). Automatic attention to emotional stimuli: Neural correlates. *Human Brain Mapping, 22*, 290-299.

Carver, C. S., & Scheier, M. F. (1998). *On the self-regulation of behavior*. New York: Cambridge University Press.

Cohen, J. D., MacWhinney, B., Flatt, M., & Provost, J. (1993). Psyscope: A new graphic interactive environment for designing psychology experiments. *Behavioral Research Methods, Instruments, and Computers, 25*, 257-271.

Cook, I. A., Bookheimer, S. Y., Mickes, L., Leuchter, A. F., & Kumar, A. (in press). Aging and brain activation with working memory tasks: An fMRI study of connectivity. *International Journal of Geriatric Psychiatry*.

Critchley, H. D., Elliott, R., Mathias, C. J., & Dolan, R. J. (2000). Neural activity relating to generation and representation of galvanic skin conductance responses: A functional magnetic resonance imaging study. *Journal of Neuroscience, 20*, 3033-3040.

Critchley, H. D., Wiens, S., Rotshtein, P., Öhman, A., & Dolan, R. J. (2004). Neural systems supporting interoceptive awareness. *Nature Neuroscience, 7*, 189-195.

Croxson, P. L., Johansen-Berg, H., Behrens, T. E. J., Robson, M. D., Pinsk, M. A., Gross, C. G., Richter, W., Richter, M. C., Kastner, S., & Rushworth, M. F. S. (2005). Quantitative investigation of connections of the prefrontal cortex in the human and macaque using probabilistic diffusion tractography. *Journal of Neuroscience, 25*, 8854-8866.

Das, P., Kemp, A. H., Flynn, G., Harris, A. W. F., Liddell, B. J., Whitford, T. J., Peduto, A., Gordon, E., & Williams, L. M. (2007). Functional disconnections in the direct and indirect amygdala pathways for fear processing in schizophrenia. *Schizophrenia Research, 90*, 284-294.

Das, P., Kemp, A. H., Liddell, B. J., Brown, K. J., Olivieri, G., Peduto, A., Gordon, E., & Williams, L. M. (2005). Pathways for fear perception: Modulation of amygdala activity by thalamo-cortical systems. *NeuroImage, 26*, 141-148.

de Marco, G., de Bonis, M., Vrignaud, P., Henry-Feugeas, M. C., & Peretti, I. (2006). Changes in effective connectivity during incidental and intentional perception of fearful faces. *NeuroImage, 30*, 1030-1037.

Demaree, H. A., Schmeichel, B. J., Robinson, J. L., Pu, J., Everhart, D. E., & Berntson, G. G. (2006). Up- and down-regulating facial disgust: Affective, vagal, sympathetic, and respiratory consequences. *Biological Psychology, 71*, 90-99.

Devinsky, O., Morrell, M. J., & Vogt, B. A. (1995). Contributions of anterior cingulate cortex to behaviour. *Brain, 118*, 279-306.

di Pellegrino, G., Ciaramelli, E., & Ladavas, E. (2007). The regulation of cognitive control following rostral anterior cingulate cortex lesion in humans. *Journal of Cognitive Neuroscience, 19*, 275-286.

Dillon, D. G., & LaBar, K. S. (2005). Startle-modulation during conscious emotion regulation is arousal-dependent. *Behavioral Neuroscience, 119*, 1118-1124.

Dolcos, F., Kragel, P., Wang, L., & McCarthy, G. (2006). Role of the inferior frontal cortex in coping with distracting emotions. . *Neuroreport, 17*, 1591-1594.

Dolcos, F., & McCarthy, G. (2006). Brain systems mediating cognitive interference by emotional distraction. *Journal of Neuroscience, 26*, 2072-2079.

Eippert, F., Viet, R., Weiskopf, N., Birbaumer, N., & Anders, S. (in press). Regulation of emotional responses elicited by threat-related stimuli. *Human Brain Mapping*.

Elliot, R., Rubinsztein, J. S., Sahakian, B., & Dolan, R. J. (2000). Selective attention to emotional stimuli in a verbal go/no-go task: An fMRI study. *Neuroreport, 11*, 1739-1744.

Fassbender, C., Murphy, K., Foxe, J. J., Wylie, G. R., Javitt, D. C., Robertson, I. H., & Garavan, H. (2004). A topography of executive functions and their interactions revealed by functional magnetic resonance imaging. *Cognitive Brain Research, 20*, 132-143.

Feldman Barrett, L., Lane, R. D., Sechrest, L., & Schwartz, G. E. (2000). Sex differences in emotional awareness. *Personality and Social Psychology Bulletin, 26*, 1027-1035.

Friston, K. J. (1994). Functional and effective connectivity: A synthesis. *Human Brain Mapping, 2*, 56-78.

Garavan, H., Hester, R., Murphy, K., Fassbender, C., & Kelly, C. (2006). Individual differences in the functional neuroanatomy of inhibitory control. *Brain Research, 1105*, 130-142.

Gilboa, A., Winocur, G., Grady, C. L., Hevenor, S. J., & Moscovitch, M. (2004). Remembering our past: Functional neuroanatomy of recollection of recent and very remote personal events. *Cerebral Cortex, 14*, 1214-1225.

Giuliani, N. R., & Gross, J. J. (in press). Reappraisal. In D. Sander & K. R. Scherer (Eds.), *Oxford companion to the affective sciences*. New York: Oxford University Press.

Goldin, P. R., Hutcherson, C. A. C., Ochsner, K. N., Glover, G. H., Gabrieli, J. D. E., & Gross, J. J. (2005). The neural bases of amusement and sadness: A comparison of block contrast and subject-specific emotion intensity regression approaches. *NeuroImage, 27*, 26-36.

Goldin, P. R., McRae, K., Ramel, W., & Gross, J. J. (in press). The neural bases of emotion regulation: Reappraisal and suppression of negative emotion. *Biological Psychiatry*.

Greenberg, D. L., Rice, H. J., Cooper, J. J., Cabeza, R., Rubin, D. C., & LaBar, K. S. (2005). Co-activation of the amygdala, hippocampus and inferior frontal gyrus during autobiographical memory retrieval. *Neuropsychologia, 43*, 659-674.

Gross, J. J. (1998a). Antecedent- and response-focused emotion regulation: Divergent consequences for experience, expression, and physiology. *Journal of Personality and Social Psychology, 74*, 224-237.

Gross, J. J. (1998b). The emerging field of emotion regulation: An integrative review. *Review of General Psychology, 2*, 271-299.

Gross, J. J., & John, O. P. (2003). Individual differences in two emotion regulation processes: Implications for affect, relationships, and well-being. *Journal of Personality and Social Psychology, 85*, 348-362.

Gur, R. C., Harper Mozley, L., Mozley, D. P., Resnick, S. M., Karp, J. S., Alavi, A., Arnold, S. E., & Gur, R. E. (1995). Sex differences in regional cerebral glucose metabolism during a resting state. *Science, 267*, 528-531.

Habel, U., Klein, M., Kellermann, T., Shah, N. J., & Schneider, F. (2005). Same or different? Neural correlates of happy and sad mood in healthy males. *NeuroImage, 26*, 206-214.

Hadjikhani, N., & de Gelder, B. (2003). Seeing fearful body expressions activates the fusiform cortex and amygdala. *Current Biology, 13*, 2201-2205.

Hariri, A. R., Bookheimer, S. Y., & Mazziotta, J. C. (2000). Modulating emotional responses: Effects of a neocortical network on the limbic system. *Neuroreport, 11*, 43-48.

Hutcherson, C. A., Goldin, P. R., Ochsner, K. N., Gabrieli, J. D. E., Feldman Barrett, L., & Gross, J. J. (2005). Attention and emotion: Does rating emotion alter neural responses to amusing and sad films? *NeuroImage, 27*, 656-668.

Jackson, D. C., Malmstadt, J. R., Larson, C. L., & Davidson, R. J. (2000). Suppression and enhancement of emotional responses to unpleasant pictures. *Psychophysiology, 37*, 515-522.

Jackson, D. C., Mueller, C. J., Dolski, I., Dalton, K. M., Nitschke, J. B., Urry, H. L., Rosenkranz, M. A., Ryff, C. D., Singer, B. H., & Davidson, R. J. (2003). Now you feel it, now you don't: Frontal brain electrical asymmetry and individual differences in emotion regulation. *Psychological Science, 14*, 612-617.

Jonides, J., Smith, E. E., Marshuetz, C., Koeppe, R. A., & Reuter-Lorenz, P. A. (1998). Inhibition in verbal working memory revealed by brain activation. *Proceedings of the National Academy of Sciences of the United States of America, 95*, 8410-8413.

Kerns, J. G., Cohen, J. D., MacDonald, A. W., III, Cho, R. Y., Stenger, V. A., & Carter, C. S. (2004). Anterior cingulate conflict monitoring and adjustments in control. *Science, 303*, 1023-1026.

Kilpatrick, L. A., Zald, D. H., Pardo, J. V., & Cahill, L. F. (2006). Sex-related differences in amygdala functional connectivity during resting conditions. *NeuroImage, 30*, 452-461.

Kim, H., Somerville, L. H., Johnstone, T., Alexander, A. L., & Whalen, P. J. (2003). Inverse amygdala and medial prefrontal cortex responses to surprised faces. *Neuroreport, 14*, 2317-2322.

Kim, H., Somerville, L. H., Johnstone, T., Polis, S., Alexander, A. L., Shin, L. M., & Whalen, P. J. (2004). Contextual modulation of amygdala responsivity to surprised faces. *Journal of Cognitive Neuroscience, 16*, 1730-1745.

Koriat, A., Melkman, R., Averill, J. R., & Lazarus, R., S. (1972). The self-control of emotional reactions to a stressful film. *Journal of Personality 40*, 601-619.

Kotter, R. (2004). Online retrieval, processing, and visualization of primate connectivity data from the cocomac database. *Neuroinformatics, 2*, 127-144.

Kumari, V., Mitterschiffthaler, M. T., Teasdale, J. D., Malhi, G. S., Brown, R. G., Giampietro, V., Brammer, M. J., Poon, L., Simmons, A., Williams, S. C. R., Checkley, S. A., & Sharma, T. (2003). Neural abnormalities during cognitive generation of affect in treatment-resistant depression. *Biological Psychiatry, 54*, 777-791.

Landro, N. I., Stiles, T. C., & Sletvold, H. (2001). Neuropsychological function in nonpsychotic unipolar major depression. *Neuropsychiatry, Neuropsychology, & Behavioral Neurology, 14*, 233-240.

Lane, R. D., Reiman, E. M., Ahern, G. L., Schwartz, G. E., & Davidson, R. J. (1997). Neuroanatomical correlates of happiness, sadness, and disgust. *American Journal of Psychiatry, 154*, 926-933.

Lane, R. D., Reiman, E. M., Axelrod, B., Yun, L.-S., Holmes, A., & Schwartz, G. E. (1998). Neural correlates of levels of emotional awareness: Evidence of an interaction between emotion and attention in the anterior cingulate cortex. *Journal of Cognitive Neuroscience, 10*, 525-535.

Lang, P. J., Bradley, M. M., & Cuthbert, B. (2001). *International affective picture system (IAPS): Instruction manual and affective ratings.* Gainseville: University of Florida, Center for Research in Psychophysiology.

Lazarus, R. S., Opton, E. M., Nomikos, S. M., & Rankin, N. O. (1965). The principle of short-circuiting of threat: Further evidence. *Journal of Personality, 33*, 622-635.

LeDoux, J. E. (1996). *The emotional brain: The mysterious underpinnings of emotional life*. New York, NY: Simon & Schuster.

Mayberg, H. S., Liotti, M., Brannan, S. K., McGinnis, S., Mahurin, R. K., Jerabek, P. A., Silva, J. A., Tekell, J. L., Martin, C. C., Lancaster, J. L., & Fox, P. T. (1999). Reciprocal limbic-cortical function and negative mood: Converging pet findings in depression and normal sadness. *American Journal of Psychiatry, 156*, 675-682.

Mayberg, H. S., Lozano, A. M., Voon, V., McNeely, H. E., Seminowicz, D., Hamani, C., Schwalb, J. M., & Kennedy, S. H. (2005). Deep brain stimulation for treatment-resistant depression. *Neuron, 45*, 651-660.

McIntosh, A. R. (1999). Mapping cognition to the brain through neural interactions. *Memory, 7*, 523-548.

McIntosh, A. R., Bookstein, F. L., Haxby, J. V., & Grady, C. L. (1996). Spatial pattern analysis of functional brain images using partial least squares. *NeuroImage, 3*, 143-157.

McIntosh, A. R., & Gonzales-Lima, F. (1994). Structural equation modeling and its application to network analysis in functional brain imaging. *Human Brain Mapping, 2*, 2-22.

McRae, K., Reiman, E. M., Fort, C. L., Chen, K., & Lane, R. D. (under review). Activity in dorsal anterior cingulate cortex during emotional arousal covaries with level of emotional awareness.

Miyake, A., Friedman, N. P., Emerson, M. J., Witzki, A. H., Howerter, A., & Wager, T. D. (2000). The unity and diversity of executive functions and their contributions to complex "frontal lobe" tasks: A latent variable analysis. *Cognitive Psychology, 41*, 49-100.

Morris, J. S., Öhman, A., & Dolan, R. J. (1999). A subcortical pathway to the right amygdala mediating "unseen" fear. *Proceedings of the National Academy of Sciences of the United States of America, 96*, 1680-1685.

Naccache, L., Dehaene, S., Cohen, L., Habert, M.-O., Guichart-Gomez, E., Galanaud, D., & Willer, J.-C. (2005). Effortless control: Executive attention and conscious feeling of mental effort are dissociable. *Neuropsychologia, 43*, 1318-1328.

Nolen-Hoeksema, S., & Jackson, B. (2001). Mediators of the gender difference in rumination. *Psychology of Women Quarterly, 25*, 37-47.

Nyberg, L., Persson, J., Habib, R., Tulving, E., McIntosh, A. R., Cabeza, R. E., & Houle, S. (2000). Large scale neurocognitive networks underlying episodic memory. *Journal of Cognitive Neuroscience, 12*, 163-173.

Ochsner, K. N., Bunge, S. A., Gross, J. J., & Gabrieli, J. D. (2002). Rethinking feelings: An fMRI study of the cognitive regulation of emotion. *Journal of Cognitive Neuroscience, 14*, 1215-1229.

Ochsner, K. N., & Gross, J. J. (2005). The cognitive control of emotion. *Trends in Cognitive Sciences, 9*, 242.

Ochsner, K. N., Ray, R. D., Cooper, J. C., Robertson, E. R., Chopra, S., Gabrieli, J. D. E., & Gross, J. J. (2004). For better or for worse: Neural systems supporting the cognitive down- and up- regulation of negative emotion. *NeuroImage, 23*, 483-499.

Öngür, D., Ferry, A. T., & Price, J. L. (2003). Architectonic subdivision of the human orbital and medial prefrontal cortex. *The Journal of Comparative Neurology, 460*, 425-449.

Paquette, V., Levesque, J., Mensour, B., Leroux, J.-M., Beaudoin, G., Bourgouin, P., & Beauregard, M. (2003). "Change the mind and you change the brain": Effects of cognitive-behavioral therapy on the neural correlates of spider phobia. *NeuroImage, 18*, 401-409.

Paradiso, S., Johnson, D. L., Andreasen, N. C., O'Leary, D. S., Watkins, G. L., Boles Ponto, L. L., & Hichwa, R. D. (1999). Cerebral blood flow changes associated with attribution of emotional valence to pleasant, unpleasant, and neutral visual stimuli in a pet study of normal subjects. *American Journal of Psychiatry, 156*, 1618-1629.

Penny, W. D., Stephan, K. E., Mechelli, A., & Friston, K. J. (2004). Modelling functional integration: A comparison of structural equation and dynamic causal models. *NeuroImage, 23*, S264-S274.

Phan, K. L., Fitzgerald, D. A., Nathan, P. J., Moore, G. J., Uhde, T. W., & Tancer, M. E. (2005). Neural substrates for voluntary suppression of negative affect: A functional magnetic resonance imaging study. *Biological Psychiatry, 57*, 210-219.

Phan, K. L., Wager, T. D., Taylor, S. F., & Liberzon, I. (2002). Functional neuroanatomy of emotion: A meta-analysis of emotion activation studies in PET and fMRI. *NeuroImage, 16*, 331-348.

Phelps, E. A., O'Connor, K. J., Gatenby, J. C., Gore, J. C., Grillon, C., & Davis, M. (2001). Activation of the left amygdala to a cognitive representation of fear. *Nature Neuroscience, 4*, 437-441.

Phillips, M. L., Drevets, W. C., Rauch, S. L., & Lane, R. (2003). Neurobiology of emotion perception I: The neural basis of normal emotion perception. *Biological Psychiatry, 54*, 504-514.

Porrino, L., Crane, A., & Goldman-Rakic, P. (1981). Direct and indirect pathways from the amygdala to the frontal lobe in rhesus monkeys. *Journal of Computational Neurology, 198*, 121-136.

Posner, M. I., & Rothbart, M. K. (1998). Attention, self-regulation and consciousness. *Philosophical Transactions of the Royal Society of London B: Biological Sciences, 353*, 1915-1927.

Preston, A. R., Thomason, M. E., Ochsner, K. N., Cooper, J. C., & Glover, G. H. (2004). Comparison of spiral-in/out and spiral-out BOLD fMRI at 1.5 and 3 T. *NeuroImage, 21*, 291-301.

Protzner, A. B., & McIntosh, A. R. (2006). Testing effective connectivity changes with structural equation modeling: What does a bad model tell us? *Human Brain Mapping, 27*, 935-947.

Ray Li, C.-S., Huang, C., Constable, R. T., & Sinha, R. (2006). Imaging response inhibition in a stop-signal task: Neural correlates independent of signal monitoring and post-response processing. *Journal of Neuroscience, 26*, 186-192.

Ray, R. D., McRae, K., Ochsner, K. N., & Gross, J. J. (under review). Cognitive up- and down-regulation of negative affect: Converging evidence from EMG and self-report.

Rubia, K., Smith, A. B., Brammer, M. J., & Taylor, E. (2003). Right inferior prefrontal cortex mediates response inhibition while mesial prefrontal cortex is responsible for error detection. *NeuroImage, 20*, 351-358.

Sabatinelli, D., Bradley, M. M., Fitzsimmons, J. R., & Lang, P. J. (2005). Parallel amygdala and inferotemporal activation reflect emotional intensity and fear relevance. *NeuroImage, 24*, 1265-1270.

Sanfey, A. G., Rilling, J. K., Aronson, J. A., Nystrom, L. E., & Cohen, J. D. (2003). The neural basis of economic decision-making in the ultimatum game. *Science, 300*, 1755-1758.

Schafer, A., Schienle, A., & Vaitl, D. (2005). Stimulus type and design influence hemodynamic responses towards visual disgust and fear elicitors. *International Journal of Psychophysiology, 57*, 53-59.

Schienle, A., Stark, R., Walteri, B., Blecker, C., Ott, U., Kirsch, P., G., S., & Vaitl, D. (2002). The insula is not specifically involved in disgust processing: An fMRI study. *Neuroreport, 13*, 2023-2026.

Seminowicz, D. A., Mayberg, H. S., McIntosh, A. R., Goldapple, K., Kennedy, S., Segal, Z., & Rafi-Tari, S. (2004). Limbic-frontal circuitry in major depression: A path modeling metanalysis. *NeuroImage, 22*, 409.

Siegle, G. J., Ghinassi, F., & Thase, M. E. (in press). Neurobehavioral therapies in the 21st century: Summary of an emerging field and an extended example of cognitive control training for depression. *Cognitive Therapy and Research*.

Smith, A. P. R., Stephan, K. E., Rugg, M. D., & Dolan, R. J. (2006). Task and content modulate amygdala-hippocampal connectivity in emotional retrieval. *Neuron, 49*, 631-638.

Somerville, L. H., Kim, H., Johnstone, T., Alexander, A. L., & Whalen, P. J. (2004). Human amygdala responses during presentation of happy and neutral faces: Correlations with state anxiety. *Biological Psychiatry, 55*, 897-903.

Spence, D. P., Lugo, M., Youdin, R. (1972). Cardiac change as a function of attention to and awareness of continuous verbal text. *Science, 176*, 1344-1346.

Taylor, S. E., Eisenberger, N. I., Saxbe, D., Lehman, B. J., & Lieberman, M. D. (2006). Neural responses to emotional stimuli are associated with childhood family stress. *Biological Psychiatry, 60*, 296-301.

Taylor, S. F., Phan, K. L., Decker, L. R., & Liberzon, I. (2003). Subjective rating of emotionally salient stimuli modulates neural activity. *NeuroImage, 18*, 650-659.

Teasdale, J. D., Howard, R. J., Cox, S. G., Ha, Y., Brammer, M. J., Williams, S. C. R., & Checkley, S. A. (1999). Functional MRI study of the cognitive generation of affect. *American Journal of Psychiatry, 156*, 209-215.

Thibodeau, R., Jorgensen, R. S., & Kim, S. (2006). Depression, anxiety, and resting frontal EEG asymmetry: A meta-analytic review. *Journal of Abnormal Psychology, 115*, 715-729.

Tsukiura, T., Fujii, T., Takahashi, T., Xiao, R., Inase, M., Iijima, T., Yamadori, A., & Okuda, J. (2001). Neuroanatomical discrimination between manipulating and maintaining processes involved in verbal working memory; a functional MRI study. *Cognitive Brain Research, 11*, 13-21.

Tugade, M. M., & Fredrickson, B. L. (2004). Resilient individuals use positive emotions to bounce back from negative emotional experiences. *Journal of Personality and Social Psychology, 86*, 320-333.

Urry, H. L., van Reekum, C. M., Johnstone, T., Kalin, N. H., Thurow, M. E., Schaefer, H. S., Jackson, C. A., Frye, C. J., Greischar, L. L., Alexander, A. L., & Davidson, R. J. (2006). Amygdala and ventromedial prefrontal cortex are inversely coupled during regulation of negative affect and predict the diurnal pattern of cortisol secretion among older adults. *Journal of Neuroscience, 26*, 4415-4425.

Vaitl, D., Schienle, A., & Stark, R. (2005). Neurobiology of fear and disgust. *International Journal of Psychophysiology, 57*, 1-4.

Veiel, H. O. (1997). A preliminary profile of neuropsychological deficits associated with major depression. *Journal of Clinical and Experimental Neuropsychology, 19*, 587-603.

Wager, T. D., Phan, K. L., Liberzon, I., & Taylor, S. F. (2003). Valence, gender, and lateralization of functional brain anatomy in emotion: A meta-analysis of findings from neuroimaging. *NeuroImage, 19*, 513-531.

Weiland-Fiedler, P., Erickson, K., Waldeck, T., Luckenbaugh, D. A., Pike, D., Bonne, O., Charney, D. S., & Neumeister, A. (2004). Evidence for continuing neuropsychological impairments in depression. *Journal of Affective Disorders, 82*, 253-258.

Weissman, D. H., Gopalakrishnan, A., Hazlett, C. J., & Woldorff, M. G. (2005). Dorsal anterior cingulate cortex resolves conflict from distracting stimuli by boosting attention toward relevant events. *Cerebral Cortex*, 229-237.

Whalen, P. J., Kagan, J., Cook, R. G., Davis, F. C., Kim, H., Polis, S., McLaren, D. G., Somerville, L. H., McLean, A. A., Maxwell, J. S., & Johnstone, T. (2004). Human amygdala responsivity to masked fearful eye whites. *Science, 306*, 2061-.

Whalen, P. J., Rauch, S. L., Etcoff, N. L., McInerney, S. C., Lee, M. B., & Jenike, M. A. (1998). Masked presentations of emotional facial expressions modulate amygdala activity without explicit knowledge. *Journal of Neuroscience, 18*, 411-418.

Williams, L. M., Barton, M. J., Kemp, A. H., Liddell, B. J., Peduto, A., Gordon, E., & Bryant, R. A. (2005). Distinct amygdala-autonomic arousal profiles in response to fear signals in healthy males and females. *NeuroImage, 28*, 618-626.

Williams, L. M., Das, P., Liddell, B. J., Kemp, A. H., Rennie, C. J., & Gordon, E. (2006). Mode of functional connectivity in amygdala pathways dissociates level of awareness for signals of fear. *Journal of Neuroscience, 26*, 9264-9271.

Wrase, J., Klein, S., Gruesser, S. M., Hermann, D., Flor, H., Mann, K., Braus, D. F., & Heinz, A. (2003). Gender differences in the processing of standardized emotional visual stimuli in humans: A functional magnetic resonance imaging study. *Neuroscience Letters, 348*, 41-45.

Wright, C. I., Martis, B., Shin, L. M., Fischer, H., & Rauch, S. L. (2002). Enhanced amygdala responses to emotional versus neutral schematic facial expressions. . *Neuroreport, 13*, 785-790.

Wright, P., He, G., Shapira, N. A., Goodman, W. K., & Liu, Y. (2004). Disgust and the insula: fMRI responses to pictures of mutilation and contamination. *Neuroreport, 15*, 2347-2351.

Yeung, N., Nystrom, L. E., Aronson, J. A., & Cohen, J. D. (2006). Between-task competition and cognitive control in task switching. *Journal of Neuroscience, 26*, 1429-1438.

Zald, D. H. (2003). The human amygdala and the emotional evaluation of sensory stimuli. *Brain Research Reviews, 41*, 88-123.